

**EFFECTS OF DEFORMATION
PROCESS ON RESIDUAL STRESS AND GRAIN
SIZE OF MAGNESIUM ALLOY ZK60**

SYUFIQA NURFATIN BINTI RASID

**RESEARCH REPORT SUBMITTED TO THE FACULTY OF
ENGINEERING UNIVERSITY OF MALAYA, IN PARTIAL
FULFILMENT OF THE REQUIREMENTS FOR THE DEGREE OF
MASTER OF MANUFACTURING ENGINEERING**

2018

UNIVERSITY OF MALAYA
ORIGINAL LITERARY WORK DECLARATION

Name of Candidates: Syufiq Nurfatina Binti Rasid

Registration/Matric No: KQG160005

Name of Degree: Master Degree

Title of Project/Research Report: Effects of Deformation Process on Residual Stress and Grain Size of Magnesium Alloy

Field of Study: Manufacturing

I do solemnly and sincerely declare that:

- (1) I am the sole author/writer of this Work;
- (2) This work is original;
- (3) Any use of any work in which copyright exists was done by way of fair dealing and for permitted purpose and any excerpt or extract from, or reference to or reproduction of any copyright work has been disclosed expressly and sufficiently and the title of the Work and its authorship have been acknowledged in this Work;
- (4) I do not have any actual knowledge nor do I ought reasonably to know that the making of this work constitutes an infringement of any copyright work;
- (5) I hereby assign all and every rights in copyright to this Work to the University of Malaya ("UM"), who henceforth shall be owner of the copyright in this Work and any reproduction or use in any form or by any means whatsoever is prohibited without the written consent of UM having been first had and obtained;
- (6) I am fully aware that if in the course of making this Work I have infringed any copyright whether intentionally or otherwise, I may subject to legal action or any other action as may be determined by UM.

Candidate's Signature

Date:

Subscribed and solemnly declared before,

Witness's Signature

Date:

Name:

Designation:

ABSTRACT

This research investigates the residual stresses and grain sizes of Parallel Tubular Channel Angular Pressing process (PTCAP) sample of 1,2 and 3 passes. PTCAP process is one of the new severe plastic deformation process (SPD) that is suitable for deforming cylindrical tubes to extremely large strains. Each sample will be under the same procedures. X-ray diffraction (XRD) measurement technique is adopted in this research as it is one of the most commonly used residual stress measurement technique. The $\sin^2\Psi$ method is used to analyze the result accordingly. Meanwhile, Electro Discharge Machining (EDM) is used to cut the samples to fit inside the XRD machine. One peak angle of 2θ at the range 55° to 59° is evaluated accordingly. The same peak angle is also used to determine the grain size by applying Scherrer Equation and SEM analysis together with EDX. The results showed that the residual stresses for each sample varies randomly. The highest residual stress is 1659.2KN which occurred on sample of 2nd pass. Meanwhile for the grain size, it keeps increasing until the sample of 3rd pass. In this experiment, the grain size does not show any correlation with residual stress of the sample as the grain size increases while residual stress varies randomly.

ACKNOWLEDGEMENTS

First of all, I would like to extend my gratitude and thanks to my great supervisor, Assoc. Professor Ir Dr Bushroa binti Abd Razak for her guidance and continues and endless support and also all the helpful advice throughout the course of this project research. N

A very special thanks towards all my colleges and University Malaya Staff who willing to help me through thick and thin. Not to forget to the most kind and helpful technician, Miss Fasharina Azreen from Faculty of Science (Geology Department) who is helping me to conduct the experiment from the beginning to the end. Also, to Mr. Mohsen who provided and prepare us the samples for the experiment.

Last but not least, my sincere appreciation to my family members and friends who gave me support endlessly. I really hope that my contribution for this research project benefits us and give opportunity for us to keep learning and develop ourselves.

TABLE OF CONTENTS

ABSTRACT	3
ACKNOWLEDGEMENTS	4
TABLE OF CONTENTS	5
LIST OF FIGURE	7
LIST OF TABLES	9
CHAPTER 1: INTRODUCTION	10
1.1 Background	10
1.2 Problem of statement	14
1.3 Objectives	14
1.4 Scope of the project	14
1.5 Organizational of the report	15
CHAPTER 2: LITERATURE REVIEW	16
2.1 X-ray Diffraction (XRD)	16
2.2 Sin2 ψ technique	19
2.3 Warren Averbach method	22
2.4 Williamson Hall Method	26
2.5 Finite Element Analysis	32
2.6 Sample cutting	36
2.7 Grain Size	39
CHAPTER 3: METHODOLOGY	41
3.1 Introduction	42
3.2 Sample preparation	42
3.3 Stress Measurement technique	44
3.4 Grain Measurement	52
3.4.1 Scherer Equation	52
3.4.2 SEM and EDX	53
CHAPTER 4 : RESULTS AND DISSCUSSION	57
4.1 Residual Stress	57
4.1.1 Experimental results	57
4.1.2 Analysis and discussion	59
4.2 Grain Size	63

4.2.1 Grain size calculated result- Scherrer Method	63
4.2.2 Grain size analysis and discussion	64
4.2.3 Grain size observed result – SEM and EDX	65
4.2.4 SEM and EDX result analysis	69
4.2.5 Grain size observed vs calculated	70
CHAPTER 5 : CONCLUSION AND RECOMMENDATION	73
REFERENCES	74

University of Malaya

LIST OF FIGURE

Figure 2. 1 Interference of x-ray beam (Moore, 2008) -----	17
Figure 2. 2 Schematic showing diffraction planes parallel to the surface and at an angle $\phi\psi$. Note σ_1 and σ_2 both lie in the plane of the specimen surface (Fitzpatrick, 2005) -----	20
Figure 2. 3 Example of a d vs $\sin^2\psi$ plot (Fitzpatrick,2005) -----	21
Figure 2. 4 Real part of the Fourier transform for family direction [0 1 0] for sample with nominal 200 Å crystallite size (Marinkovic et.al, 2001) -----	22
Figure 2. 5XRD pattern of the uncharged (without H) and cathodic hydrogenated DSS for 72 h and aged at RT for different time intervals (0 h, 1 h, 2 h, 4 h, 6 h, and 1 month) (Silverstein and Eliezer, 2017)-----	28
Figure 2. 6XRD pattern of the uncharged (without H) and gas-phase hydrogenated DSS for 5 h at 50 MPa and 200 °C, after aging for one month at RT) (Silverstein and Eliezer, 2017)-----	29
Figure 2. 7 Comparison between (a) hardness mapping and (b) equivalent plastic deformation calculated by FEA for the cross-section of the ECAPed sample (Reyez et.al, 2016) -----	33
Figure 2. 8Experimental and numerical temperature history at every four quadrants (left), temperature contour plot and fusion boundaries (right) (Hemmes et.al, 2017) -	34
Figure 2. 9 Short model in the self-balanced state after loading of residual stresses (Meng et.al,2015) -----	35
Figure 2. 10Distributions of near-surface residual stresses for 5 surface conditions (Schajer, 2013) -----	38
Figure 3. 1 Sample 1 pass of PTCAP -----	43
Figure 3. 2 Sample 2 passes of PTCAP -----	43
Figure 3. 3 Sample 3 passes of PTCAP -----	43

Figure 3. 4 PANalytical XRD Machine -----	44
Figure 3. 5 (a) and (b) Sample placed on the tool holder -----	45
Figure 3. 6 Sample rack inside the machine -----	46
Figure 3. 7 (a) and (b) Absolute Scan setting and graph -----	47
Figure 3. 8 Setting for the stress measurement program -----	49
Figure 3. 9 (a) and (b) The measurement of scan result -----	51
Figure 3. 10 (a) and (b) XRD scan and FWHM value for each peak from absolute scan -----	53
Figure 4. 1 Graph d vs. $\sin^2\Psi$ for sample 1 pass.....	57
Figure 4. 2 Graph d vs. $\sin^2\Psi$ for sample 2 passes.....	58
Figure 4. 3 Graph d vs. $\sin^2\Psi$ for sample 3 passes.....	58
Figure 4. 4 Residual Stress Measurement.....	59
Figure 4. 5 XRD profile of Magnesium Alloy ZK60 (Mater et.al, 2009)	63
Figure 4. 6 SEM PTCAP 1 pass.....	66
Figure 4. 7 EDX acquisition graph PTCAP 1 pass.....	66
Figure 4. 8 SEM PTCAP 2 passes	67
Figure 4. 9 EDX acquisition graph PTCAP 2 pass.....	67
Figure 4. 10 SEM PTCAP 3 passes	68

LIST OF TABLES

Table 3. 1 XRD measurement parameters -----	50
Table 4. 1 Residual Stress Measurement Value -----	59
Table 4. 2 Grain size measurement -----	64
Table 4. 3 Grain size calculated value -----	64
Table 4. 4 EDX PTCAP 1 pass -----	66
Table 4. 5 EDX PTCAP 2 pass -----	67
Table 4. 6 EDX PTCAP 3 pass -----	68
Table 4. 7 EDX acquisition graph PTCAP 3 pass -----	68
Table 4. 8 Grain size difference -----	70

CHAPTER 1: INTRODUCTION

1.1 Background

Recently, there has been quite numbers of interest in enhancing the material performance using severe plastic deformation (SPD) technique such as Parallel Tubular Channel Angular Pressing (PTCAP) process. This method was initially originated as a pattern by Faraji in 2011. It is suitable to process a tube to a very high strain. In the beginning of the research, it was demonstrated and processed by using Magnesium Alloy. In year 2016, Mesbah et.al continue the research by using the same technique to characterize the nano mechanical properties of pure UFG Brass tube. Since Brass are widely used in the industries such as automotive and aerospace manufacturing, there is need to further the research and use the advantage from this process. In this process, the tube is constrained by inner and outer dies and eventually will be pressed down by a hollow cylindrical punch with 2 shear zones in the middle. This procedure increase the micro hardness significantly and also changed the structure as it elongate the sub grain. It also build the radial tensile and compressive strain. Hence, the deformation may cause unwanted residual stress into the tube. The unwanted residual stress may lead to harm as it can affect the tool life and tool performance in the future.

Tavakkoli et.al (2015) also used the same PTCAP method to study the severe mechanical anisotropy of high strength UFG Cu-Zn tube. It is proven that this method show improvement in their yield strength from ~106 MPa to ~344 MPa in axial direction and ~359-1013 MPa in peripheral direction. Meanwhile back in 2012, the effect number of passes on grain refinement and dislocation density were studied by Faraji et.al (2013) on the sample of copper tube produced by PTCAP method. Multiple number of passes were performed and the result showed that the sub grain only elongated extensively at the first pass. However, at second and third pass, the sub grain elongation decrease. It shows

that by increasing the number of passes will decrease the dislocation densities. Besides, Sanati et.al (2014) employed PTCAP method to evaluate the residual stress in ultrafine-grained in aluminum tube by using shearography technique. It claimed that by increasing the number of passes of PTCAP, it will decrease the number of the residual stress and the stress gradient become lower. They also did an evaluation by using finite element analysis. The results showed that the stress distribution stop changing after the 3rd passes.

Residual stress can be defines as the stress that remain in the material when the external force is absence. The stress still remain inside the material after the external force is removed. There are several factors that can cause residual stress. One of the cause is from the process used to make the components itself. For instance, the manufacturing and fabrication process like welding, molding, plastic deformation, bending, rolling etc. Among the factors that are known to cause residual stresses are the development of deformation gradients in various sections of the piece by the development of thermal gradients, volumetric changes arising during solidification or from solid state transformations, and from differences in the coefficient of thermal expansion in pieces made from different materials (Withers, 2007). The presence of residual stress can cause lots of things such as a visible distortion to the component or can cause the components to a sudden split at an idle condition. Residual stress is an important factor in order for us to enhance or maximize the mechanical properties of an object. Usually, compressive stress is more desired compared to tensile stress as it strengthen the material itself. Meanwhile, for the tensile residual stress considered to be harmful as it can lead to severe fatigue strength and bad mechanical properties of the material. As the residual stress is hard to see, it need a very reliable method of measurement with a minimum damage to the surface. Thus, the correct type of residual stress measurement is required.

There are lots of residual stress measuring techniques has been developed by researcher or scientist. There are three main type of measuring techniques; destructive

measurement, semi-destructive measurement and non-destructive measurement. The application of these techniques depends on certain factor. For instance, material used, practical issues or measurement issues. Selection of the correct method of measurement is important as we do not want to distort or change the original residual stress in the material. Due to that, most of the researcher prefer to use non-destructive method as we can directly measure the residual stress. However, there are some limitation like the size of the material is too big, or the location of the material itself can not fit the measuring table area. Due to that, semi-destructive method is proposed either to do drilling method, counterboring method or slitting method.

One of the most applicable method of non-destructive method of measurement is x-ray diffraction method also known as XRD. By using XRD the stress level and strain can be measured. This technique of measurement able to measure the residual stress up to stress to depth up to 30 μm by measuring the materials inter-atomic spacing. Besides its non-destructive mechanism, it also quite versatile, widely used, and able to measure micro and macro residual stress. Instead of using destructive method, non-destructive method is employed as it has very minimal risk to interrupt the location of residual stress. Besides, we need to consider the process itself so it not the stress that already occur, or else it may lead the development of bigger residual stress. Non-destructive method also helps to maintain the quality of workpiece. Lots of aspects that can take into account in order to choose the most suitable method for measurement. There are practical issues, material issues and the measurement characteristic itself. Hemmesi, Farajian and Boin (2017) conducted a studies of residual stress in tubular joints by using x-ray and diffraction analysis. From the study, they found that both method were very suitable and useful to measure residual stresses either in axial or hoop direction. Meanwhile, lots of other study like Meng et.al (2015), Lee et.al(2015) and Foadian et.al (2016) also use the

same method of residual stress measurement as it able to penetrate to the desire depth, can help to define the atomic structure and commonly used method.

In order to analyze the result of the measurement, few approaches can be employed. The most common is finite element analysis. By using this method, we can see the different between the actual measurement results with the simulation result. Simulation can be done by using any FEA software like Abaqus or Ansys. The three-dimensional model of the present work is developed by Solid Work and the corresponding residual stress will be calculate by means of FEM. All parameters and mechanical loading will be included and simulation will be performed. Sometimes, it is hard to only depend on the experimental value itself as has lots of other influence factors. For instance, pure experimental residual stress measurement cannot describe quantitatively the influence of each parameters, aside from being too expensive or not applicable for certain cases like huge or complicated structure of workpiece. The other most common method is sin²psi method. The crystallographic planes tilted surface normal at different psi angle. The lattice spacing depends on the strain in the elasticity strained crystalline material. While for Williamson-Hall method, it employ the principle of approximation formula for the size broadening. In this particular method, size broadening and strain broadening will be respect to Bragg's angle. The absolute value for this approach cannot be taken seriously. However it can be very useful if used in relative sense. Warren Averbach could be considered as a very precise and accurate method to analyze the residual stress measurement. It adopt the deconvulation of Fouries-Transformation (also known as Stokes Method) for determination of physical line profile.

By analyzing the residual stress result using all these methods, we can compare and see the reliability of each method, hence determine the residual stress of the material accordingly.

1.2 Problem of statement

PTCAP is one of the SPD process which helps to enhance the properties of material. The process itself involved a tube that been constrained by inner and outer dies, pressed by hollow cylindrical punch into the tubular angular channel with 2 shear zones. This process proven to elongate sub grain hence able to increase the micro hardness eventually. The process gave the additional tensile and compressive strain because the diameter of the tube change during the process and revert to the initial state at the end.

Throughout the process, the radial tensile and compressive strain is built as the process increase the number of passes. PTCAP is one of the methods that can develop shear deformation which can cause considerable residual stress into the tube material. Hence, accurate stress strain calculation acting upon the tube material need to be measured.

1.3 Objectives

The main aim of this research is to measure the residual stress of the tube material that already undergoes PTCAP deformation process. Besides, the other objectives are:

1. To determine maximum load applied in the PTCAP
2. To calculate and compared the grain sizes between the Scherrer Method and SEM image

1.4 Scope of the project

In this project, three sample of Magnesium Alloy ZK60 will be investigated under X-ray Diffraction Machine to see their residual stress and also their crystallite size. All the sample were prepared earlier by using one of the severe plastic deformation method

which is Parallel Tubular Angular Chanel Pressing Process (PTCAP). These three sample has different number of passes; 1, 2 and 3 passes.

1.5 Organizational of the report

Chapter one describe briefly on the background of the project. It explained on how the tube material is processed initially. In this project, the same material is going to be used to measure the residual stress by using XRD technique. The statement of problem also being included showing the main issue of this project. The objective is determined and this experiment will be conducted within the scope selected.

Meanwhile in chapter two, the literature review is conducted by showing the result of previous research on related topics. It is including the text of scholarly papers explain about all the method of analysis of residual stress measurement like sin square psi method, Warren Averbach method, Williamson Hall method and finite element analysis. Also included the best way to prepare the sample for the XRD measurement.

Chapter three involve the methodology of this project. All the method used starting from the sample preparation to the grain size measurement procedure. Followed by chapter four where all the result being presented and analyzed. Finally the last chapter covers the overall conclusion and also some recommendation in order to improve the result for future research.

CHAPTER 2: LITERATURE REVIEW

This chapter covers the literature review conducted in the fields of residual stress measurement by using XRD technique.

2.1 X-ray Diffraction (XRD)

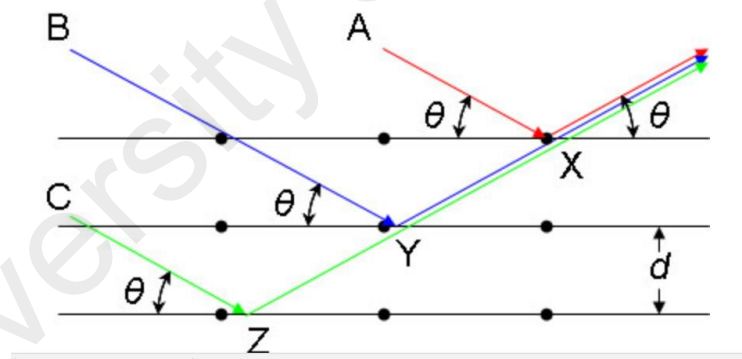
X-ray diffraction method (XRD) has been recognized as a powerful technique to determine residual stress as well as to characterize the internal structure and mechanical state of crystalline material. It also can be employed to analyze the bulk microstructure. The residual stress that produce the strain is calculated by assuming a linear elastic distortion of the crystal lattice. It able to measure either macroscopic or microscopic stresses nondestructively.

This technique to measure residual stress to depth up to 30 μ m by measuring the materials inter-atomic spacing. Laboratory X-rays have wavelengths of the order of a few angstroms (\AA), which is the same order of magnitude as the typical inter-atomic/inter-planar distances in polycrystalline solids. X-rays scattered from a polycrystalline solid can constructively interfere producing a diffracted beam. The angles at which the maximum diffracted intensities occur are measured. From these angles it is possible to obtain the inter-planar spacing, d , of the diffraction planes using Bragg's law. If residual stresses exist within the sample, then the d spacing will be different from that of an unstressed sample (i.e. d_0). The difference is proportional to the magnitude of residual stress present. In principle therefore, we use the grains as internal strain gauges for residual (or applied) stresses (Fitzpatrick, 2005).

Bragg's law is applied in x-ray diffraction method. Basically, the XRD machine calculate the distance between the atoms. Bragg's Law was introduced by Sir W.H. Bragg and his son Sir W.L. Bragg. The law states that when the x-ray is incident onto a crystal surface, its angle of incidence, θ , will reflect back with a same angle of

scattering, 2θ . And, when the path difference, $d\sin\theta$ is equal to a whole number, $n\lambda$, of wavelength, a constructive interference will occur. Consider a single crystal with aligned planes of lattice points separated by a distance d . Monochromatic X-rays A, B, and C are incident upon the crystal at an angle θ . They reflect off atoms X, Y, or Z. The path difference between the ray reflected at atom X and the ray reflected at atom Y can be seen to be $2d\sin\theta$. From the Law of Sine we can express this distance YX in terms of the lattice distance and the X-ray incident angle. If the path difference is equal to an integer multiple of the wavelength, then X-rays A and B (and by extension C) will arrive at atom X in the same phase. In other words, given the following conditions:

Then the scattered radiation will undergo constructive interference and thus the crystal will appear to have reflected the X-radiation. If, however, this condition is not satisfied, then destructive interference will occur.



$$n\lambda = 2d\sin\theta$$

Figure 2. 1 Interference of x-ray beam (Moore, 2008)

where:

- λ is the wavelength of the x-ray,
- d is the spacing of the crystal layers (path difference),
- θ is the incident angle (the angle between incident ray and the scatter plane), and
- n is an integer

The principle of Bragg's law is applied in the construction of instruments such as Bragg spectrometer, which is often used to study the structure of crystals and molecules (Moore, 2008).

There are many of researcher used XRD to measure residual stress. For instance Hensi et.al (2017) has conducted a research on measuring the welding residual stress by means of two technique; x-ray and neutron diffraction method. These two methods were adopted to assess how residual stresses are distributed in the material, especially in the critical crack initiation sites. The accuracy for both side is influenced by the several assumption and simplification. They agreed to use both of these method as this experiment involve their own none fully limitation. Bragg's principle describe the determination of residual stresses on the basis of diffraction theories. By comparing the result with the computer simulation, the overall agreement is good accept for some discrepancies in the surface and subsurface stress result over the weld area. Combining these two methods give a good residual stress profile towards the bulk material.

Meanwhile, Meng et.al (2015) used XRD method in conjunction to determine surface residual stress of Ti6Al4V tubes and study the effect of different machining parameters. As the residual stress induced by machining can lead to distortion of dimensional accuracy and fatigue life of workpiece, it is crucial to know the residual stress build up in the material and choose the right way of measurement, so the initial stress still remain and the most commonly method is x-ray diffraction. However, in the experiment they combined XRD with layer removal method. Because the residual stress are redistributed and a new self-balanced state is attained after the removal of each layer, the residual stress in a newly exposed surface layer is altered, especially in a workpiece of low rigidity. Hence, the stress values obtained by the XRD method require correction to determine the actual initial stresses by using finite element correction method.

Equal Channel Angular Pressing (ECAP) process is one of the Severe Plastic Deformation (SPD) technique to improve material properties that quite similar with TCAP. The shear deformation may lead to residual stress distribution at the bulk and surface of the sample. The author claimed that there is no quantitative study on stress distribution on sample processed by ECAP. Hence they employed XRD as one of the method to measure the residual stress. The analysis was carried out by means of conventional and high energy X-Ray diffraction (synchrotron) to the surface. By using XRD, the residual stresses of the surface able to be analyzed and compared with other method.

2.2 Sin2 ψ technique

In residual stress measurement by using X-ray diffraction (XRD), it measure the strain in the crystal lattice hence determine the associated residual stress from the elastic constants. It is done by assuming a linear elastic distortion of the suitable crystal lattice plane. Many grain crystal will contribute in measurement. Although the measurement is considered to be near surface, X-rays do penetrate some distance into the material: the penetration depth is dependent on the anode, material and angle of incidence. Hence the measured strain is essentially the average over a few microns depth under the surface of the specimen.

In order to perform strain measurement, the sample must be exposed to the x-ray beam that will interact with crystal lattice. The strain within the surface of the material can be measured by comparing the unstressed lattice inter-planar spacing with the strained inter-planar spacing. This, however, requires precise measurement of an unstrained sample of the material. By altering the tilt of the specimen, measurements of planes at an angle ψ can be made and thus the strains along that direction can be calculated using

$$\varepsilon_{\psi} = \frac{d_{\phi\psi} - d_0}{d_0} \quad (2.1)$$

Figure shows planes parallel to the surface of the material and planes at an angle $\phi\psi$ to the surface. This illustrates how planes that are at an angle to the surface are measured by tilting the specimen so that the planes are brought into a position where they will satisfy Bragg's Law (Fitzpatrick, 2005).

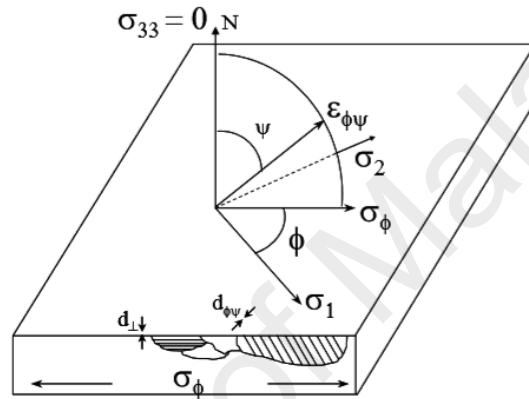


Figure 2. 2 Schematic showing diffraction planes parallel to the surface and at an angle $\phi\psi$. Note σ_1 and σ_2 both lie in the plane of the specimen surface (Fitzpatrick, 2005)

In order to measure a single stress acting in same direction in surface, Elasticity theory for an isotropic solid shows that the strain along an inclined line is as following

$$\varepsilon_{\phi\psi} = \frac{1+\nu}{E} (\sigma_1 \cos^2 \phi + \sigma_2 \sin^2 \phi) \sin^2 \psi - \frac{\nu}{E} (\sigma_1 + \sigma_2) \quad (2.2)$$

If we consider the strains in terms of inter-planar spacing, and use the strains to evaluate the stresses, then it can be shown that

$$\sigma_{\emptyset} = \frac{E}{(1+\nu)\sin^2\Psi} \left(\frac{d_{\Psi}-d_n}{d_n} \right) \quad (2.3)$$

This equation allows us to calculate the stress in any chosen direction from the inter-planar spacings determined from two measurements, made in a plane normal to the surface and containing the direction of the stress to be measured.

Sin2 ψ method is the most common method for stress determination. XRD measurements are made at many different tilt angle. The inter-planar spacing, or 2-theta peak position, is measured and plotted as a curve similar to that shown in Figure below:

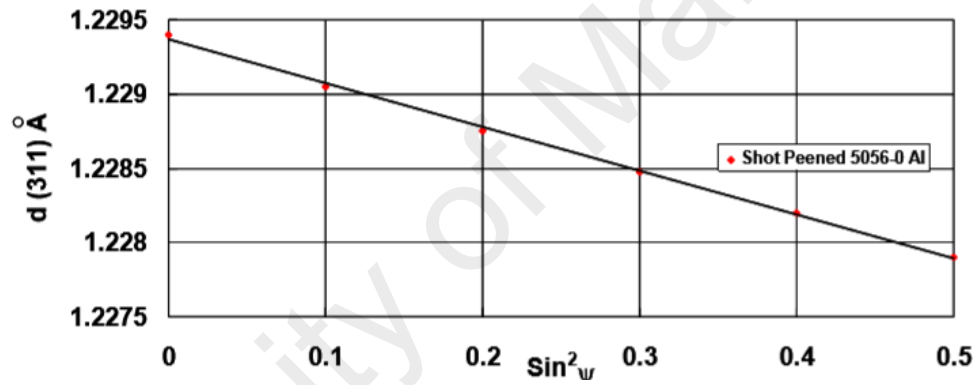


Figure 2. 3 Example of a d vs sin2 ψ plot (Fitzpatrick,2005)

The stress can then be calculated from such a plot by calculating the gradient of the line and with basic knowledge of the elastic properties of the material. This assumes a zero stress at $d = d_n$, where d is the intercept on the y-axis when $\sin^2 \psi = 0$. Thus, the stress is given by:

$$\sigma_{\emptyset} = \left(\frac{E}{1+\nu} \right) m \quad (2.4)$$

Where m is the gradient of the d vs. $\sin^2 \psi$ curve. However, this is only the basic for stress determination (Fitzpatrick, M. E ,2005).

2.3 Warren Averbach method

In year 2001, Marinkovic et.al conducted a research on comparing Warren Averbach method with other alternate method of analyzing x-ray diffraction profile. They propose to use fundamental approach to simulate the instrument contribution to the XRD profile. In this procedure, the need to prepare the reference sample is eliminated. The other alternate methods Warren Averbach been compared with are Balzar and Enzo method which is focusing on size strain analysis. In this experiment, two crystallite size are used which are 80Å and 200Å. The proposed simulation procedure is much faster compared to others. However, for larger crystallite size, Warren Averbach data are more consistent even though it is more tedious work involved. It also do not have any retriCTION to calculate multimodal distribution compared to Balzar and Enzo method used in the experiment. In fact, the size coefficient can also be determine. The limitation that been noticed is that it doesn't assume any shape of diffraction line and make no assumption about form of the peak profile.

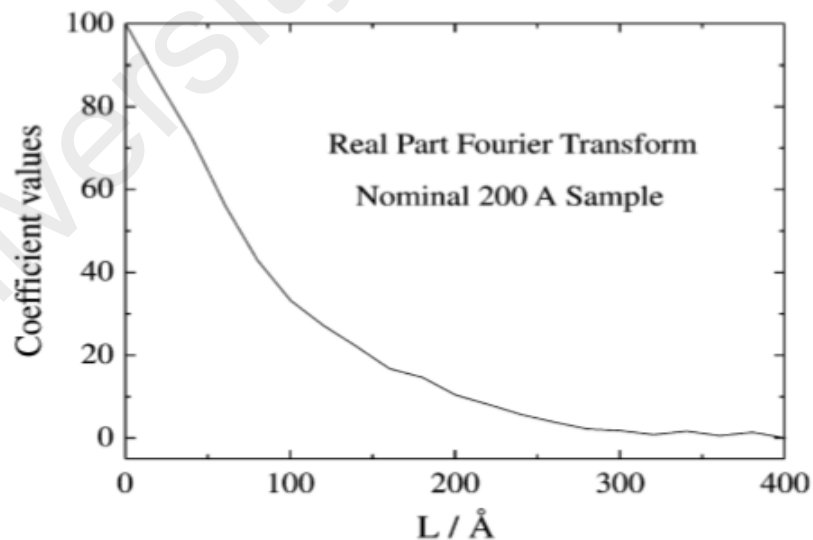


Figure 2. 4 Real part of the Fourier transform for family direction [0 1 0] for sample with nominal 200 Å crystallite size (Marinkovic et.al, 2001)

The Warren–Averbach (WA) method (zhang et.al, 2003) is based on the premise that the XRD line profile can be interpreted as a Fourier transformation of the crystalline structure in reciprocal space, or that a Bragg-peak line profile may be expressed as a Fourier series having the following form:

$$f(s) \propto \sum_{L=-\infty}^{\infty} \{A(L) \cos[2\pi(s - s_0)L] + B(L) \sin[2\pi(s - s_0)L]\} \quad (2.5)$$

where $A(L)$ and $B(L)$ are the cosine and sine Fourier coefficients, respectively, and L is the conjugate variable to $s-s_0$ in the real space and is interpreted as the column length of unit cells perpendicular to the diffracting planes corresponding to the Bragg peak. The $s = 2 \sin \theta / \lambda$ is a reciprocal variable, and the diffraction peak is assumed to be centered at s_0 . Warren[10] and McKeehan and Warren showed that the coefficient $A(L)$ can be written as the product of a size coefficient and a strain coefficient: $A(L) = A_{\text{size}}(L) A_{\text{strain}}(L)$. Likewise, due to the different dependence of $A_{\text{size}}(L)$ and $A_{\text{strain}}(L)$ on L , as mentioned previously, separation of the two coefficients can be carried out and for a cubic system it can be expressed as

$$\ln A_L(h_0) = \ln A_L^S - \frac{2\pi^2 L^2 [\epsilon_L^2]}{a^2} h_0^2 \quad (2.6)$$

Usually, measurements of the second-order peak are subjected to greater uncertainty than the first-order peak because of reduced intensity for the second-order reflection. Delhez et al.[18] pointed out a modified version less sensitive to statistical errors in determining the Fourier size coefficient A_L^S :

$$A_L(h_0) = A_L^S \left(\frac{2\pi^2 L^2 [\epsilon_L^2]}{a^2} h_0^2 \right) \quad (2.7)$$

where $L = n\lambda / (2(\sin \theta_2 - \sin \theta_1))$, $\theta_2 - \theta_1$ is the Bragg angle interval, and n is the Fourier order.[10,19] The term a is the lattice constant, $h^2 + k^2 + l^2$, and h, k , and l are the Miller indices. The term $\epsilon^2 L$ is the mean square strain perpendicular to the reflection planes. The grain size can be calculated as

$$L_a = \frac{A_L^S(0)}{\lim_{L \rightarrow 0} \left(\frac{dA_L^S}{dL} \right)} \quad (2.8)$$

where L_a is interpreted as an area averaged column length of unit cells.

Meanwhile in 2015, Hajyakbary et.al using the same method of analysis to characterize the dislocation density in lath martensitic structure. They called it an improved method of x-ray diffraction analysis. However, in this method of analysis the modified Warren Averbach (MWA) and modified Williamson Hall (MWH) method is combined. They claimed that MWH method is an accessible method in XRD line profile analysis which able to find the dislocation densities, however they need to adopt MWA method in order to find the value of dislocation distribution parameter (M). In the present work, an improved approach has been developed for XRD line profile analysis by combining the MWH and MWA methods. This approach provides an expression for the Fourier coefficients that is valid for any range of length of Fourier coefficient L .

The XRD peak broadening cause by strong strain has been used to find the dislocation density, ΔK . However, for case strong strain anisotropy, ΔK not easy to calculate as it is not a linear function. Due to that, Ungar et.al (1998) has developed a modified Warren Averbach method by taking account influence of strain anisotropy. To do this, they introduced scaling parameters C , called average contrast factor of dislocation. In MWA method, diffraction pattern measured is expressed by Fourier Series.

This combined method is developed by the fact that both modified methods give the similar value for dislocation density.

Simm et.al (2016) investigate evaluation of diffraction peak profile analysis (DPPA) methods to study plastically deformed metals. In the experiment, four metal were deformed. by uniaxial tension and compression to a range of strains. The methods we have considered include, the full-width, Williamson-Hall methods, Warren Averbach methods, and van Berkum's alternative method. Different metals were chosen to understand the effect of the deformation microstructure and crystal structure. The dislocation density values found by Williamson-Hall and Warren-Averbach methods were found to be close to those expected from TEM results of similar metals. When using the Warren-Averbach methods the results suggest that systematic errors in the dislocation density are introduced by three main factors: (1) separation of instrumental broadening, (2) separation of size and strain broadening, and (3) separation of dislocation density and arrangement. Which suggests in many cases the simpler Williamson-Hall method may be preferable.

Chen et.al (2005) use Fourier analysis of X-ray micro-diffraction profiles to characterize laser shock peened metals. By using classical Warren and Averbach method (Warren and Averbach, 1950) and its modification (Ungar and Borbely, 1998), the spatial distribution of inhomogeneous strain deviation, mosaic size and dislocation density were evaluated through Fourier analysis of X-ray micro-diffraction profiles for single crystal Al and Cu. According the work of Ungar and Borbely (1998), the analysis of Fourier coefficients of X-ray profiles shows that taking into account the dislocation effect on the profiles gives a modified method, known as the modified W–A analysis. This procedure enables a straightforward determination of dislocation density from X-ray line profile analysis. In Ungars model, for crystals containing dislocations, the diffraction profile is

also considered as the combination of the diffracted X-ray for all unit cells in crystal as that in W–A method. However, the displacement of each unit cell is represented by the dislocation Burgers vector to account for the effect of dislocation structure and the real part of the Fourier coefficients of the X-ray line profile can be written as

$$\ln A_n = c_0 - \rho^* n^2 \ln \left(\frac{R_e}{n} \right) + Q^* n^4 \ln \left(\frac{R_2}{n} \right) \ln \left(\frac{R_3}{n} \right) \quad (2.9)$$

where q^* is the “formal” dislocation density, directly available from a broadened profile without taking into account the effect caused by different types of dislocations. Q^* is given as the variation of the dislocation density, n is the harmonic number, and R_e is the outer cutoff radius of dislocations, which indicates the distribution range of dislocation stored energy. R_2 and R_3 are auxiliary constants. The true value of dislocation density is

$$\rho = \frac{2\rho^*}{\pi g^2 b^2 C} \quad (2.10)$$

Where C is the average contrast factor for different type of dislocations (edge and screw) in the case of a particular hkl reflection and can be found in Ungar and Borbely (1996), b is the Burgers vector of dislocations. Thus, after calculating the real part of the Fourier coefficients A_n , the $\ln A_n - n$ data can be fitted as non-linear curve using formula in (2.9). The parameters such as q^* can be determined in curve fitting using least-squares evaluation method and the dislocation density q can be evaluated by Eq. (2.10).

2.4 Williamson Hall Method

Wang et.al (2017) has been investigating the relaxation of residual stress and also strain hardening effect in microstructure of shot peened Ni-Al bronze at an elevated temperature. X-ray profile line analysis which is modified Williamson Hall analysis with uniform deformation energy density model was adopted. It is because taking the

anisotropy nature of crystals into account is more realistic compared with the uniform deformation model and the uniform stress deformation model. In this experiment, MWH method is used only to evaluate the changes of domain size and microstrain. Besides compressive residual stress, shot peening also lead to refinement of grain size, increase in micro strain and also dislocation density in surface layer. Prior to using modified Williamson-Hall method to evaluate the domain size and the lattice strain, the structurally broadened breadth should be separated out from the measured breadth of the corresponding diffraction peak

$$\beta_S^2 = \beta_M^2 - \beta_I^2 \quad (2.11)$$

where β_S , β_M and β_I denote the structurally broadened breadth, the measured breadth and the instrumental broadened breadth, respectively. From three modified Williamson-Hall models which are the uniform deformation model, the uniform stress deformation model and the Uniform energy deformation model (UEDM), the last one usually provides the best fitting results and is observed to be the most realistic model. In the UEDM, the density of deformation energy (u) which results in the anisotropic lattice strain is assumed to be uniform.

Meanwhile in 2017, Silverstein and Eliezer also employing Williamson Hall method in analyzing the residual stress on hydrogen trapping in duplex stainless steels. It was used to study the individual contributions of crystallite size and lattice strain on the peak broadening of DSS with and without hydrogen. The WH plot was developed for hydrogen charged sample. This method is an integral breadth analysis for X-ray lines, which is based on the fact that Bragg peaks are affected by lattice strains that increase the peak width.

Deviations from perfect crystallinity extend in all directions, which then lead to broadenings of the diffraction peaks. The crystallite size and lattice microstrain are the two main properties which could be extracted from the peak width analysis. The crystal imperfections could be measured from the distributions of lattice constants. From Figs. 2 and 3, it can be deduced that Bragg peaks were affected by the lattices' microstrain, which increase the peak width and intensity, shifting the 2θ peak position accordingly. The values of microstrain and lattice's domain size were deduced by the use of W–H equations as follows. The average domain size was calculated using Scherrer's formula for broadening $\beta = (\lambda / D) \cos\theta$ where, β is the peaks' broadening, λ is the testing wave's length, D is the average domain size, and θ is the peak's angle. The strain induced, ϵ , was calculated by $\epsilon = \beta / 4 \tan\theta$. By combining these two formula, the next equation become $\beta \cos\theta / \lambda = (1/D) + (4 \epsilon \sin\theta / \lambda)$. By plotting $\beta \cos\theta$ versus $4/\lambda \sin\theta$, microstrain and domain size can be achieved.

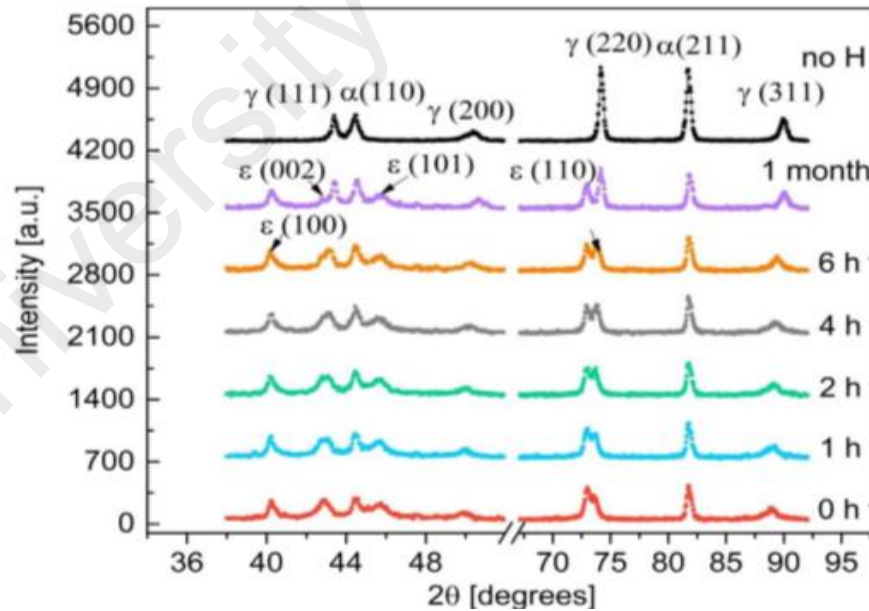


Figure 2. 5 XRD pattern of the uncharged (without H) and cathodic hydrogenated DSS for 72 h and aged at RT for different time intervals (0 h, 1 h, 2 h, 4 h, 6 h, and 1 month) (Silverstein and Eliezer, 2017)

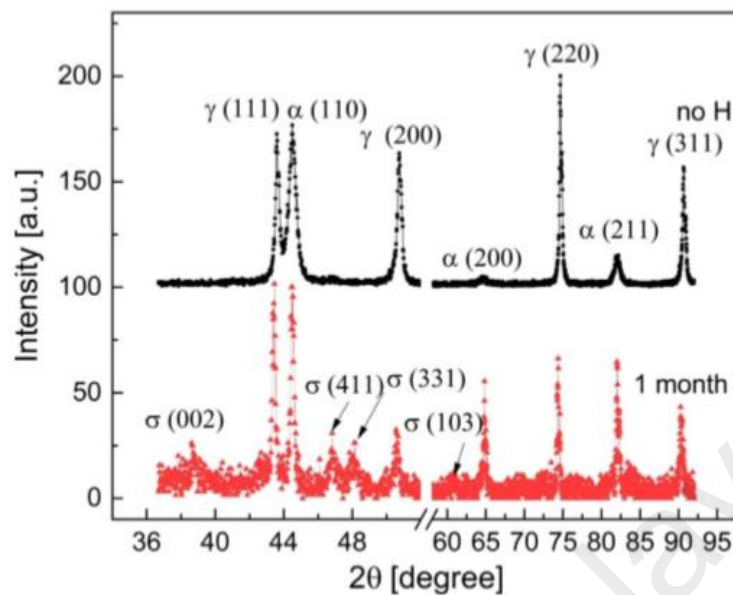


Figure 2. 6XRD pattern of the uncharged (without H) and gas-phase hydrogenated DSS for 5 h at 50 MPa and 200 °C, after aging for one month at RT) (Silverstein and Eliezer, 2017)

Williamson Hall analysis also been used by Mote et.al in year 2012 to analyze the estimation of lattice strain in nanometer sized ZnO particles. X-ray peak broadening analysis is used in order to calculate the crystalline sized and lattice strain by the Williamson Hall analysis. They claimed that this x-ray profile analysis is simple yet a powerful tool to estimate the crystallize size and lattice strain. WHM is a simplified analysis where size-induced and strain-induced broadening are deconvoluted by considering the peak width as function of 2 theta. In the latest work, a modified form of WHM is adopted, namely uniform deformation model. Other than that, there are also Uniform Deformation stress model (UDSM) and Uniform Deformation Energy Stress Model (UDESME) that help get the idea of stress strain relation. In UDM, the isotropic nature of crystal is considered while in UDESME and UDSME assume the crystal is of anisotropic nature. The result of the experiment showed that there are significant

broadening of the peak showing some evidence of grain refinement. An instrumental broadening was corrected using the relation

$$\beta_{hkl} = [(\beta_{hkl})^2_{\text{measured}} - (\beta_{hkl})^2_{\text{instrumental}}]^{1/2} \quad (2.12)$$

The average nano crystalline was calculated by using Debye Sherer's formula as following:

$$D = \frac{K\lambda}{B_{hkl} \cos\theta} \quad (2.13)$$

Where D=crystalline size, K= shape factor, and lambda is wavelength. Meanwhile for the strain induced, the crystal imperfection and distortion was calculated by using this following formula:

$$\varepsilon = \frac{B_{hkl}}{4\tan\theta} \quad (2.14)$$

By assuming particle size and strain contribution to line broadening are independent to each other having Cauchy line profile and rearranging the equation, the final equation would be:

$$B_{hkl} \cos\theta = \frac{K\lambda}{D} + 4\varepsilon \sin\theta \quad (2.15)$$

The above equation known as Williamson Hall equation. Then, the graph is plotted. This equation can be considered as Uniform deformation model (UDM) where strain can be assume to be a uniform in all the direction of crystallographic, hence assume it as isotropic crystal nature. Uniform deformation model and uniform deformation energy density model were taking into account where the anisotropic nature of Young's Modulus is more realistic. In this case, the above equation is modified and get:

$$B_{hkl}\cos\theta = \frac{K\lambda}{D} + 4\sin\theta\sigma/E_{hkl} \quad (2.15)$$

The uniform stress then can be obtained from the slope of the graph plotted using above modified equation. However, in many cases the homogeneity and isotropic is not fulfilled. Hence the equation need to be modified to the form that fulfill the certain condition.

An investigation using Williamson Hall method also used by S.Brandstetter et.al in year 2008 to investigate anisotropy in nanocrystalline in metal. XRD technique allow the determination of mean grain size root-mean square strain and dislocation peak through peak profile analysis and the Williamson Hall approach. In this procedure, only two diffraction peaks of the same crystallographic family are needed to separate the effect of grain size and rms strain on the peak broadening, when the twin density is neglected or of a known value. of the IW vs. scattering vector, an effect that is often referred to as the anisotropy in the Williamson–Hall (WH) plot. Such WH anisotropy has been interpreted in terms of a lattice dislocation and/or twin fault content. content. The introduction of dislocation contrast factors by Ungar et.al (199) has allowed the development of profile analysis procedures that can result in a quantitative determination of the dislocation density, grain size and twin density, a procedure called the modified WH analysis.

Such contrast factors provide a measure of how strongly the dislocations can affect the RMS strain within the system and thus the strain-broadened component of the Bragg diffraction peak profile. To contribute to the basic understanding of the character of the WH anisotropy in nc metals, a method to calculate the XRD profile from multi-million atom computer-simulated samples has been developed. It was shown that for

Voronoi nc networks with generally high-angle GBs and defect-free grain interiors, the calculated XRD patterns exhibit an almost linear WH plot.

Simm et.al (2016) run an investigation by applying several different methods to study plastically deformed metals. They claimed that by adopting Williamson Hall method, it produced dislocation density values more consistent with expectations than the Warren-Averbach method. The Williamson-Hall method is a popular method to determine size and strain values from the full-width or integral breadths of a diffraction pattern. The advantage of the method is that only the full-width is needed so the quality of the peaks need not be as high as in some methods. The method works by fitting straight lines to plots of the full-width (or integral breadth) against the reciprocal of the lattice spacing; the gradient gives the microstrain and the intercept the size. Different methods can be used depending on the separation of size and strain and the use of the contrast factor.

2.5 Finite Element Analysis

Finite element analysis is one of the branch of solid mechanics. Nowadays it is commonly used for multiphysics problem. FEA really helpful to compare the actual experimental result with the simulation itself. Mahur et.al (2017) did a review on finite element analysis for estimation of residual stresses in welded structures. FEA can effectively estimate residual stresses, especially the relaxation of residual stresses in weld region and region in close vicinity under repeated loading. The amount of the residual stress relaxation depends on the magnitude of applied repeated loading. In the destructive and semi-destructive, the residual stresses are measured by means of stress-relaxation i.e. by measuring the elastic-strain release induced when a sample is segmented, drilled or milled using mechanical/electrical strain gauges. Generally, resistance strain gauges, removable extensometers and photoelastic surface layers are mainly used for

measurements. Though they are destructive and semi-destructive, the stress relaxation techniques provide dependable data and are the most widely accepted and are frequently referred. In crystalline material, elastic strain can be prescribed non-destructively by evaluating lattice specification using XRD. Due to limitations of either cost or accuracy, its practical application is less. Numerical simulation based on Finite Element Analysis (FEA) offers a radical approach for the prediction of residual stress.

Meanwhile for Reytez et.al (2016), they employed FEA methods to evaluate the residual stress distribution of aluminium alloy under a shear deformation. It was found that the microhardness mapping and residual stress results showed a good agreement with the finite element analysis for the first layer studied. Three-dimensional finite elements analysis was developed using the commercial finite element code SIMULIA Abaquss, in order to compare and correlate the results obtained from the different techniques. The plastic deformation process was simulated using a die set channel similar to that used in the experimental procedure.

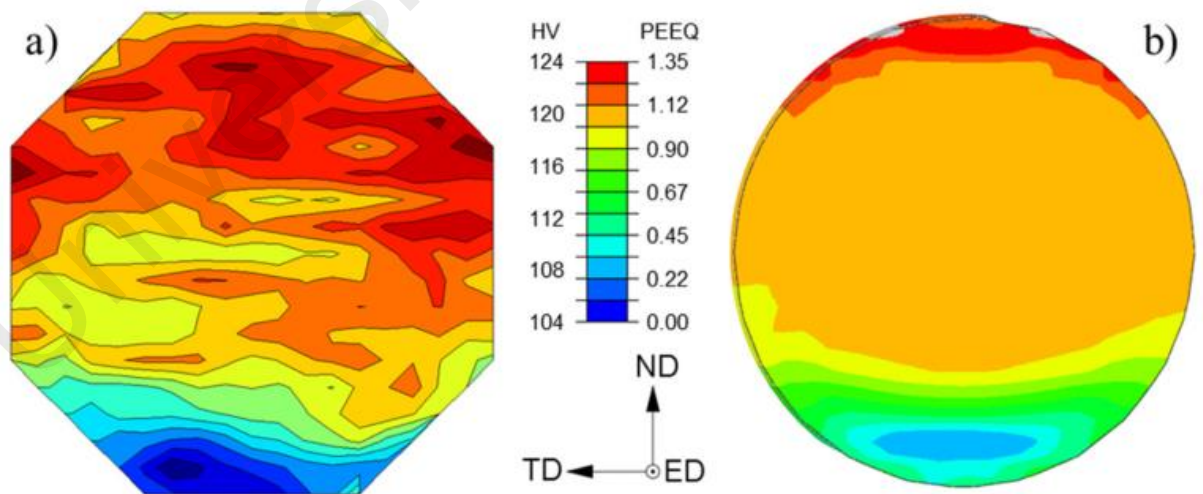


Figure 2. 7 Comparison between (a) hardness mapping and (b) equivalent plastic deformation calculated by FEA for the cross-section of the ECAPed sample (Reytez et.al, 2016)

Hemmes et.al (2016) also employing FEA method in order to find the residual stress distribution. By using FEA, it can easily determine affected area or critical area that exposed to residual stress. In this paper finite element approach is applied in order to calculate the welding residual stresses in a tube out of S355J2H steel using the commercial software package SYSWELD. For comparison with the numerical investigations x-ray and neutron diffraction measurements (XRD and ND) are carried out to determine the distribution of residual stresses in three orthogonal directions, on the surface and in the bulk of the material respectively. The numerical results are compared directly with the measured data. The overall aim is to evaluate the use of finite element approach in the accurate calculation of residual stress states for use in the integrity assessments.

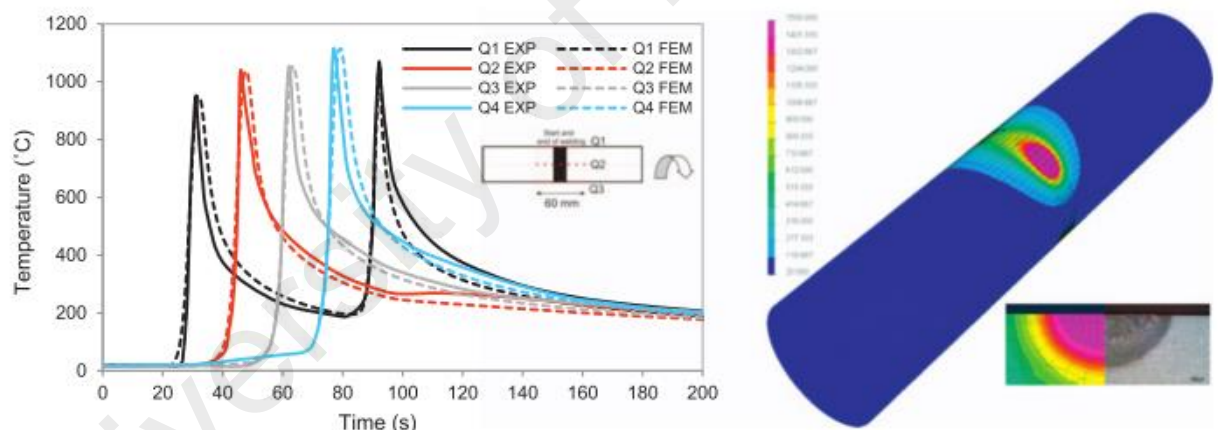
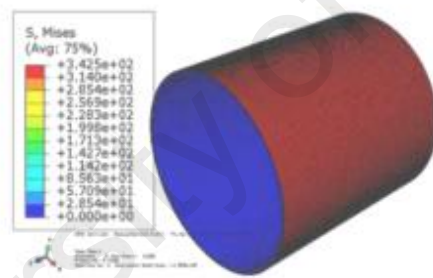


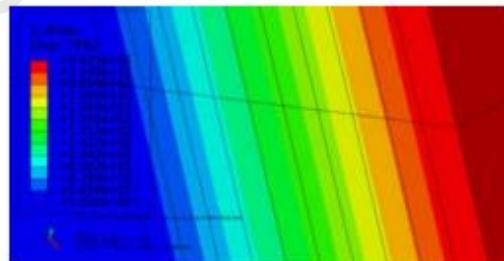
Figure 2. 8Experimental and numerical temperature history at every four quadrants (left), temperature contour plot and fusion boundaries (right) (Hemmes et.al, 2017)

Meng et.al (2015) also adopting FEA in measuring Surface Residual Stresses Generated by Turning Thin-Wall Ti6Al4V Tubes Using Different Cutting Parameters. In the present study, it is known that FEA is such a powerful and useful method determine the optimal required length of the workpiece, taking into consideration factors such as

accuracy, convenience, and materials saving. In this experiment, A new and highly accurate FEA-based correction method involving simple calculations was proposed. The method was used in conjunction with XRD to determine the surface residual stresses of Ti6Al4V tubes and analyze the effects of different turning parameters and annealing. To reduce the edge effect and obtain accurate results, the test tube should be sufficiently long. However, measurement convenience and materials saving require the tube to be short. Considering these two conflicting requirements, FEA is used to determine the optimal tube length. The finite element model of the tube was developed using Abaqus. Using the above FEA results as a guide, a model was created in Abaqus with an external diameter of 45 mm, internal diameter of 43 mm, and length of 50 mm. After loading the residual stresses on the model, a self-balanced state was attained as shown:



Complete short model in the self-balanced state



Part of the short model in the self-balanced state

Figure 2. 9 Short model in the self-balanced state after loading of residual stresses
(Meng et.al,2015)

2.6 Sample cutting

Since the tool holder for XRD machine has a very limited area, the sample must be cut to fit into the machine. However, the appropriate cutting mechanism must be selected as we do not want to disturb the initial residual stress inside the sample. Tsivoulas et.al (2015) conducted a research on effects of flow forming parameters on the development of residual stresses in Cr–Mo–V steel tubes. Residual stress generation during flow forming tubular components of Cr–Mo–V ferritic steel has been studied in detail using laboratory X-ray and neutron diffraction. In order to study the homogeneity of residual stress throughout the flow formed tube, the sample was cut by using electron discharge machining (EDM). EDM is a process that not introduce any additional stress into component when the machining is performed carefully. However, a local stress relaxation due to material removal is unavoidable.

EDM is a machining process that used to cut any conductive materials. It has the ability to machine very precisely regardless any complex and irregular shape. Any machining process that induced the residual stress on the surface may be beneficial or detrimental to machined parts. Since EDM is a non-contact machining process, it hardly induced any residual stress compared to other machining process. According to Srinivasa et.al (2016), EDM process give less detrimental effect to parts during machining. Wire EDM and sinker EDM machines were generally used for production of complex shapes of aluminum components with extremely tight tolerances in a single setup. Since there was no contact with the workpiece in EDM it produces very fine shapes that were not possible with traditional machining. Many of researcher attempted to find the effect of various factor in generation of residual stress on EDMed components. Ghanam et.al (2011) claimed that they found the tensile residual stress during the machining but can be reduced by performing polishing operation to stabilize the residual stress. Meanwhile Soo

et.al (2013) claimed that very low residual stress was observed during g machining of Ti–6Al–2Sn–4Zr–6Mo aerospace alloy in both rough and finish cut operations in wire EDM.

It is very crucial to determine the best method to cut the sample as we do not add or introduced new stress to the sample. EDM been used to cut sample for destructive method of measuring residual stress like slitting and counterering method. For instance in contour method, EDM is used to cut through specimen cross-section. Meanwhile in surface profiling, EDM is one of the readily available method besides ECM/super-polishing. However, it is noted that EDM process will produce a thin highly stressed recast layer. This layer may be very hard and hard to remove. Any material removal at a stressed specimen surface will lead to a local redistribution of stresses. This must be considered prior to any material removal. Where near-surface stress gradients are large, removal of surface material may lead to unacceptable changes in stresses. But the EDM-affected area is possible to be removed by using electropolishing.

A residual stress measurement was done by using hole drilling method. A series of holes drilling test are drilled on different condition of material surface. The material surface are wire cut EDM surface, EDM surface; recast layer removed using a fine abrasive stone, shot-peened, Shot peened followed by smoothing using a fine stone to remove peening indentations and Shot-peened and smoothed (as 4) followed by further fine abrasion.

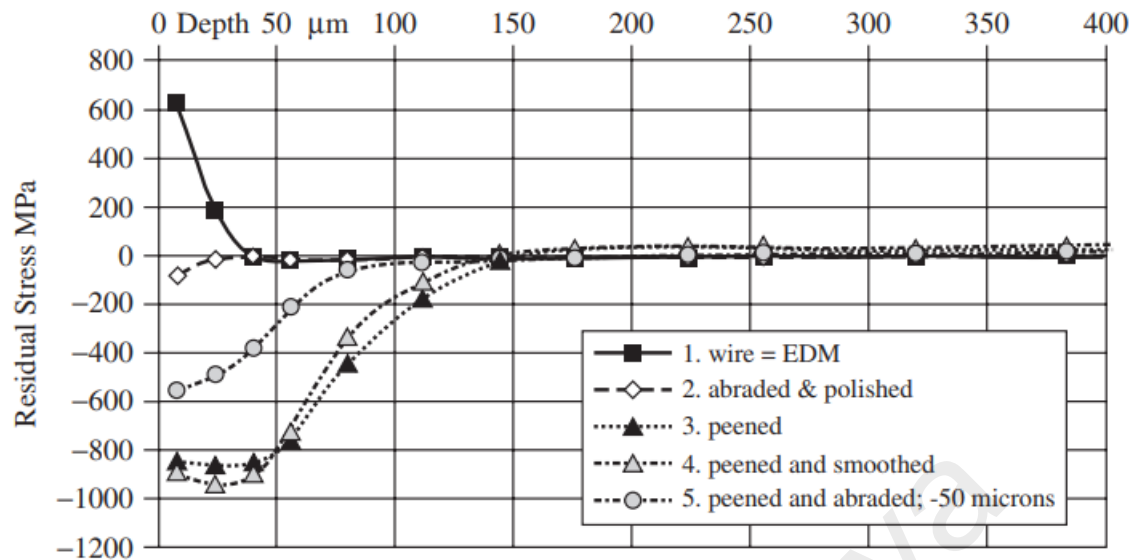


Figure 2. 10Distributions of near-surface residual stresses for 5 surface conditions

(Schajer, 2013)

From the graph in Figure 1, it shown that residual stress on surface of recast EDM has only small amount of tensile stresses within the first two calculation increments, which can subsequently be removed using a fine abrasive stone. Tests of this type are very useful for the development of surface preparation methods and parameters.

On the other hand, slitting method of measuring residual stress also employed EDM to cut the sample. it is because EDM provides good dimensional control and, since it does not rely on mechanical force, does not impose significant residual stress when cutting, if used at low material removal rates. Careful planning is required when mounting the specimen in the EDM cutting tool. Minimal clamping is generally desirable so that the sample can deform in response to stress release. The contouring method also use EDM to cut the metallic parts. Since the EDM cut width varies for different materials, irregularities in cutting maybe occurred. Local cutting irregularities, such as wire breakage or overburning at some foreign particle, are usually small length scale (order of wire diameter) and can be removed by the data smoothing process or manually from the raw data. In contouring method, EDM is currently the method of choice as it is the ideal

cutting process that has the following characteristics: a straight (planar) and cut with a smooth surface, minimal cut width (kerf), not removing any further material from already cut surfaces, and not causing any plastic deformation or inducing any residual stress.

In wire EDM, a wire is electrically charged with respect to the workpiece, and spark erosion causes material removal. The cutting is non-contact, whereas conventional machining causes localized plastic deformation from the large contact forces. The part is submerged in temperature-controlled deionized water during cutting, which minimizes thermal effects. The wire control mechanisms can achieve positional precision of a fraction of a micrometer, especially for a straight cut (Schajer, 2013).

2.7 Grain Size

Scherrer equation is an equation used in XRD to calculate and analyze the grain size of the sample. Most of the time, this method used in order to determine the grain size of particle in the powder form. Since the PTCAP process is initially started with ultrafine-grain (UFG), hence this method could be considered to use for grain size calculation.

In December 2016, Chakravarty et.al used this method to evaluate the microstructure of Nanocrystalline Cu Alloy. The sample was first scanned under XRD machine to attain the XRD pattern. From there, the value of Full Width at Half Maximum can be obtained for the individual peak.

Meanwhile, Darling et.al (2013) was investigating on the grain size stabilization of copper at high temperature. The estimation of microstructural length for each phases was done by XRD analysis corresponding to Scherrer Equation. Yi et.al (2007) also use the same method to determine the substrate grain size of NiFe film. The sample was scanned by XRD machine and grain size was calculated by using Scherrer Equation. They

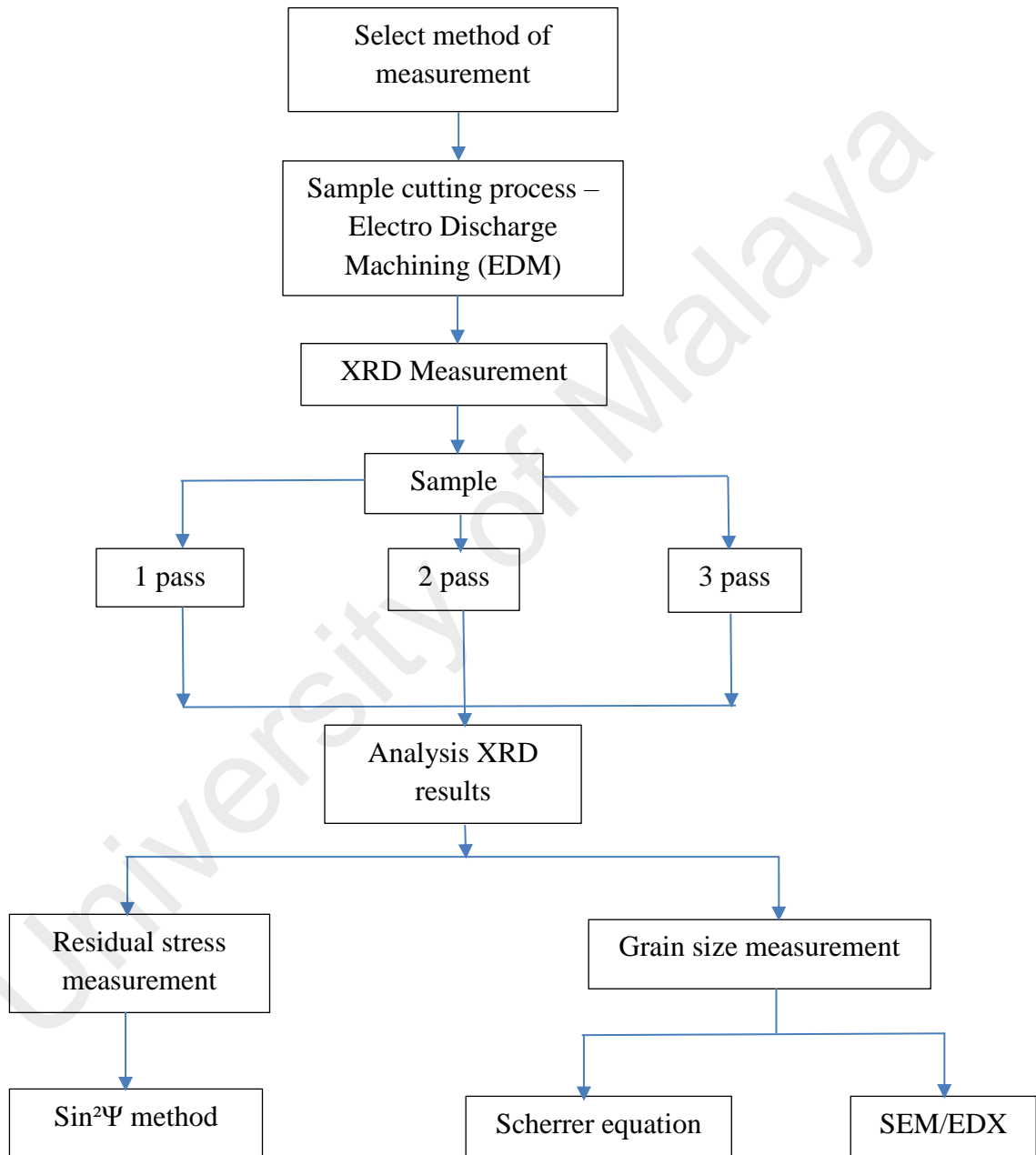
did conduct the microstructural analysis by observing the sample under the SEM to prove the calculation made earlier.

Thus, Scherrer Equation is one of the most used method and equation to determine the grain and crystallite size from the XRD measurement.

University of Malaya

CHAPTER 3: METHODOLOGY

In this chapter, a step by step procedure will be explained accordingly.



3.1 Introduction

In this project research work, three samples is prepared by Parallel Tubular Angular Chanel Pressing Process (PTCAP) will be investigated. Each of this sample varied with different number of passes; 1, 2 and 3 passes. All these samples will undergoes residual stress measurement by using one of the non-destructive technique which is X-ray Diffraction technique. Besides the residual stresses, the grain size or crystallite size also will be observed and calculated accordingly.

3.2 Sample preparation

All three samples used in this research project was already done previously by a PHD student. The sample initially was in a tube shape having a dimension of 40mm length and 20mm diameter with a hallow section in the middle. The thickness of the tube is 2.5mm. The material of the sample also all the same which is Magnesium Alloy ZK60. In order to put the sample into the XRD machine, it to be cut as it does not fit the tool holder inside the machine. The appropriate cutting technique like Electron Discharge Machining (EDM) was selected as it gave minimum amount of distortion on residual stress. It will only affect small area at the cutting zone.

Figure 3.1, 3.2 and 3.3 showed the sample that already been cut by using EDM into a small section for all three passes.



Figure 3. 1 Sample 1 pass of PTCAP



Figure 3. 2 Sample 2 passes of PTCAP



Figure 3. 3 Sample 3 passes of PTCAP

3.3 Stress Measurement technique

In this research project, XRD technique is used to measure the residual stress of the PTCAP sample. Due to some technical problem, the experiment was done in Faculty of Science at Geology Department XRD Lab. The XRD machine used is PANalytical EMPYREAN. It able to load until 10 sample in one time and do the measurement continuously. Figure 3.4 below showed the machine used in the lab.



Figure 3. 4 PANalytical XRD Machine

As the tool holder only allow limited size of sample, the smallest sample is chosen and placed neatly inside the tool holder. The sample is placed at the center and pressed onto the clay (orange) so that it can hold the sample while the x-ray beam strike the sample. This step need to be done very precisely as we want the x-ray beam to strike the desired area.



(a)



(b)

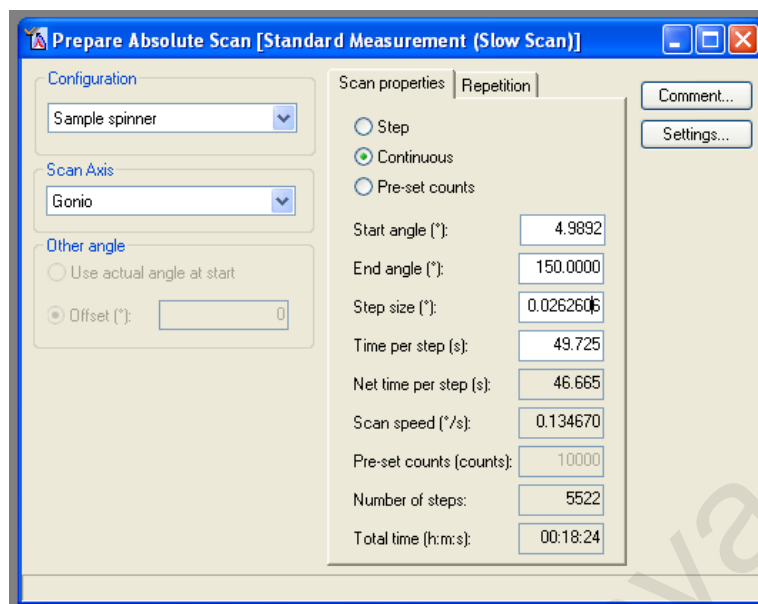
Figure 3. 5 (a) and (b) Sample placed on the tool holder

After all the samples are put in the tool holder, then all of these sample will load onto the XRD sample rack that will allow the measurement to be done continuously.

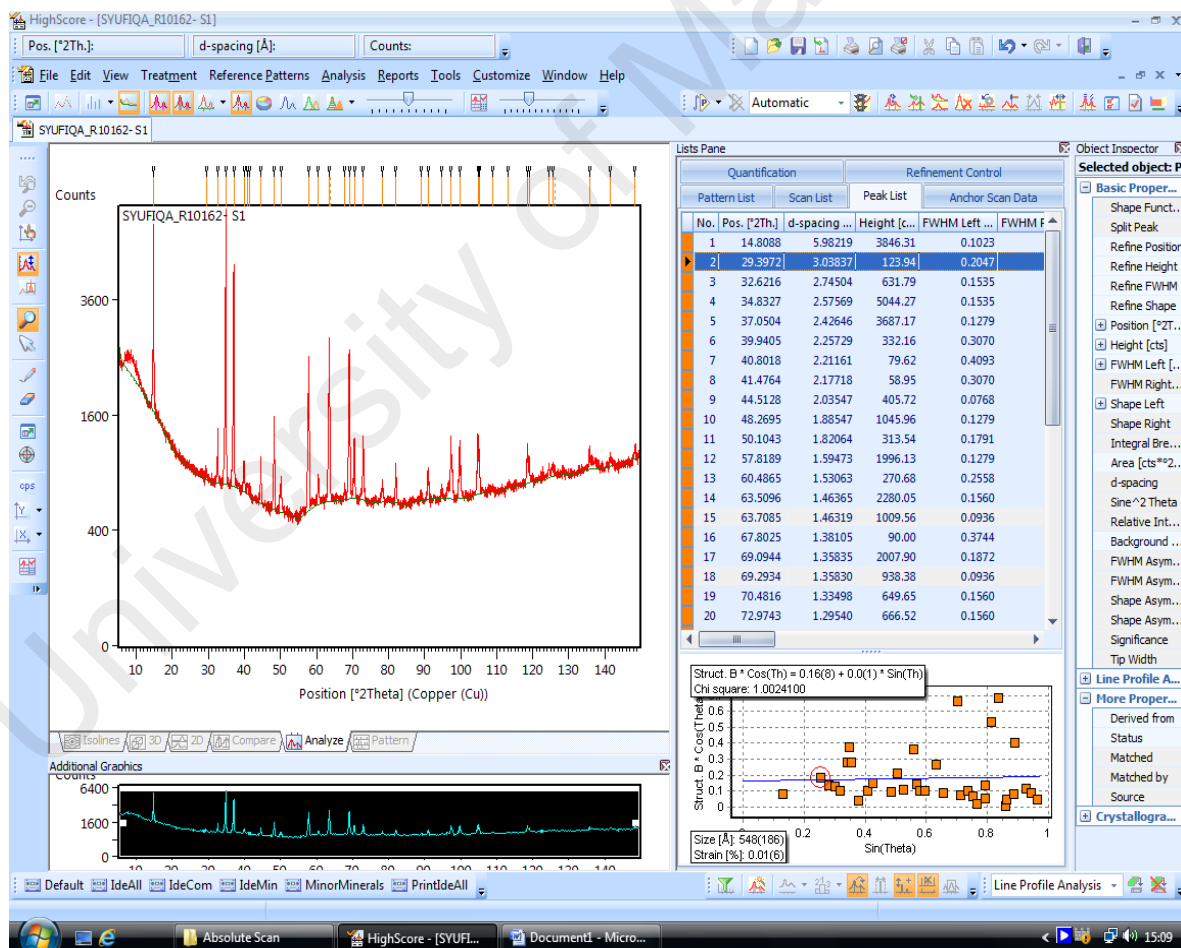


Figure 3. 6 Sample rack inside the machine

The first step in order to make residual stress measurement is to take the absolute scan for all these three sample. The purpose to take the absolute scan is to find one fixed value for 2θ and find the best peak for the stress measurement later.



(a)



(b)

Figure 3. 7 (a) and (b) Absolute Scan setting and graph

After the absolute scan is obtained, one particular peak is selected in order to proceed with the stress measurement. All the settings are selected and keyed in according to the preference. The tilt angle or $\sin^2 \psi$ angle was set in the scan table for stress program. Meanwhile ψ angle will be calculated automatically from the $\sin^2 \psi$ angle. The scan portion will be the position of the peak chosen. Others setting will be generate automatically. The modify scan table of stress program will show all the setting that has been chosen including the scanning time.

The screenshot displays the 'Prepare Stress measurement [Stress Nik mas]' window. It is organized into several sections with various input fields and buttons.

- Configuration:** Includes a dropdown for 'Sample spinner'.
- Tilt axis:** A dropdown menu set to 'Omega'.
- Tilt range:** A dropdown set to 'Positive + negative'. Below it are input fields for 'Psi limit - max. Psi (°)' (14.0000) and 'Sin2Psi step size' (0.0046).
- Phi steps:** An input field for 'No. of Phi-steps' set to 1.
- Scan axis:** A dropdown menu set to '2Theta-Omega'.
- Other gonio angle:** Radio buttons for 'Use actual angle at start' (selected) and 'Offset (°)' (0.0000).
- Scan mode:** Radio buttons for 'Step', 'Continuous' (selected), and 'Pre-set counts'.
- Range and Timing:** A series of input fields: 'Range (°)' (4.0179), 'Step size (°)' (0.0262606), 'Time per step (s)' (49.725), 'Net time per step (s)' (46.665), 'Scan speed (°/s)' (0.134670), 'Pre-set counts (counts)' (10000), and 'Number of steps' (153).
- Buttons:** 'Comment...', 'Settings...', and 'Scan Table...' are located in the top right.
- Scan positions:** A table with one row containing a play icon and the value 57.8189. A '*' icon is below it. A 'Delete selected row' button is at the bottom.
- Current scan table:** Summary statistics: 'No. of scans' (21) and 'Total time (h:m:s)' (00:19:55).

(a)

Modify Scan Table Stress Program [Stress Nik mas]

No.	Psi (°)	Sin2Psi	Phi (°)	2Theta (°) Start	2Theta (°) End	2Theta (°) Step Size	No. of steps	Time per step (s)	Net time per step	Pre-set counts	Scan time (h:m:s)
1	-12.3848	0.0460	0.0	55.8100	59.8278	0.0262606	153	49.725	46.665	10000	00:00:57
2	-11.7399	0.0414	0.0	55.8100	59.8278	0.0262606	153	49.725	46.665	10000	00:00:57
3	-11.0598	0.0368	0.0	55.8100	59.8278	0.0262606	153	49.725	46.665	10000	00:00:57
4	-10.3374	0.0322	0.0	55.8100	59.8278	0.0262606	153	49.725	46.665	10000	00:00:57
5	-9.5630	0.0276	0.0	55.8100	59.8278	0.0262606	153	49.725	46.665	10000	00:00:57
6	-8.7230	0.0230	0.0	55.8100	59.8278	0.0262606	153	49.725	46.665	10000	00:00:57
7	-7.7960	0.0184	0.0	55.8100	59.8278	0.0262606	153	49.725	46.665	10000	00:00:57
8	-6.7463	0.0138	0.0	55.8100	59.8278	0.0262606	153	49.725	46.665	10000	00:00:57
9	-5.5041	0.0092	0.0	55.8100	59.8278	0.0262606	153	49.725	46.665	10000	00:00:57
10	-3.8890	0.0046	0.0	55.8100	59.8278	0.0262606	153	49.725	46.665	10000	00:00:57
11	0.0000	0.0000	0.0	55.8100	59.8278	0.0262606	153	49.725	46.665	10000	00:00:57
12	3.8890	0.0046	0.0	55.8100	59.8278	0.0262606	153	49.725	46.665	10000	00:00:57
13	5.5041	0.0092	0.0	55.8100	59.8278	0.0262606	153	49.725	46.665	10000	00:00:57
14	6.7463	0.0138	0.0	55.8100	59.8278	0.0262606	153	49.725	46.665	10000	00:00:57
15	7.7960	0.0184	0.0	55.8100	59.8278	0.0262606	153	49.725	46.665	10000	00:00:57
16	8.7230	0.0230	0.0	55.8100	59.8278	0.0262606	153	49.725	46.665	10000	00:00:57
17	9.5630	0.0276	0.0	55.8100	59.8278	0.0262606	153	49.725	46.665	10000	00:00:57
18	10.3374	0.0322	0.0	55.8100	59.8278	0.0262606	153	49.725	46.665	10000	00:00:57
19	11.0598	0.0368	0.0	55.8100	59.8278	0.0262606	153	49.725	46.665	10000	00:00:57
20	11.7399	0.0414	0.0	55.8100	59.8278	0.0262606	153	49.725	46.665	10000	00:00:57
21	12.3848	0.0460	0.0	55.8100	59.8278	0.0262606	153	49.725	46.665	10000	00:00:57

OK Cancel Sort Insert Delete Help

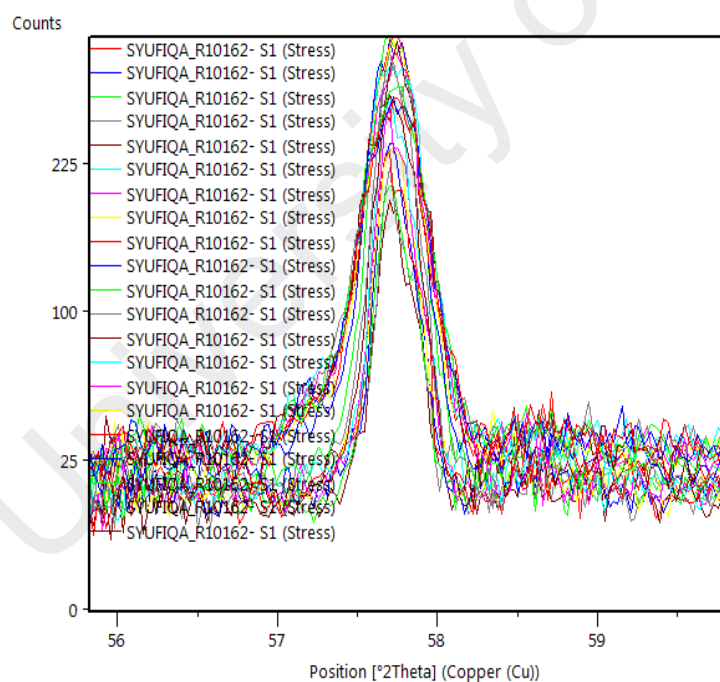
(b)

Figure 3. 8 (a) and (b) Setting for the stress measurement program

Based on the scan, the value of d-spacing was taken for different tilt angle in order to calculate the residual stress using the elasticity theory. These parameters are chosen based on the peak angle which start from 55.810° and end at 59.8278°. The others parameters were automatically calculated once the range and peak angle is insert. Meanwhile for the parameters for tube voltage and tube current for stress measurement are fixed at 40 kV and 40 mA. The value of d-spacing is taken from the peak list for every scan list. The table below showed the residual stress measurement parameters used in this experiment.

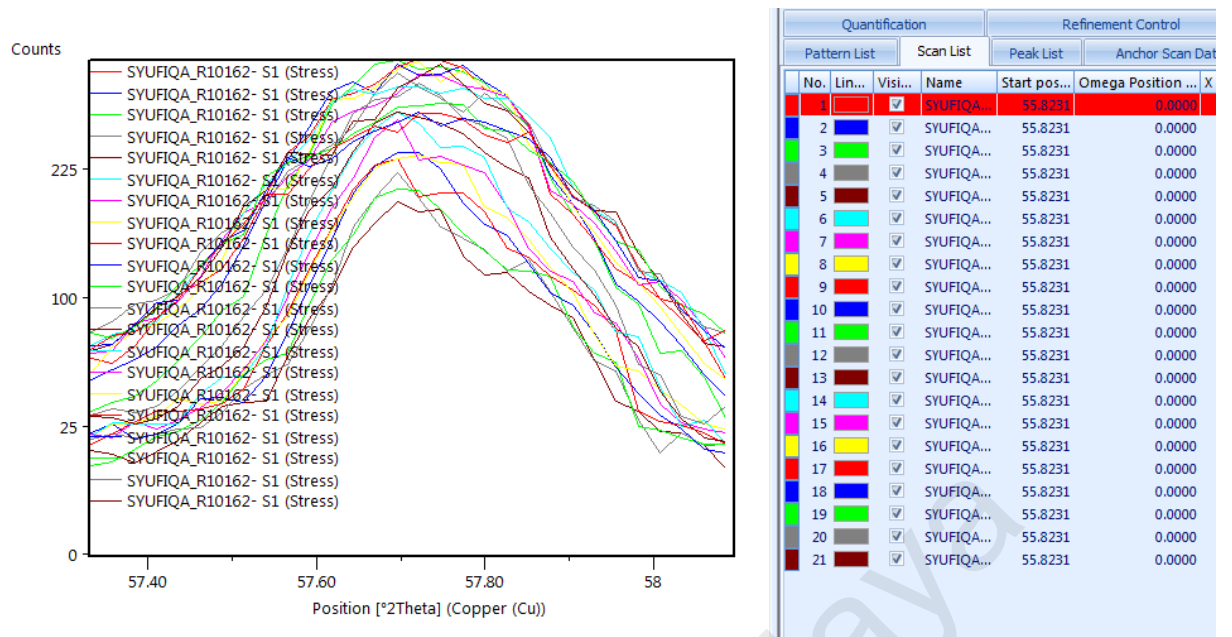
Table 3. 1 XRD measurement parameters

Measurement method	Sin2 Ψ
Target	Cu K α
Tube voltage (kV)	40
Tube current (mA)	40
Peak of 2theta (°)	58.8199
Start angle (°)	55.8100
Stop angle (°)	59.8278
Ψ (°)	$\pm(12.3848, 11.7399, 11.0598, 10.3374, 9.563, 8.723, 7.796, 6.7643, 5.5041, 3.8890, 0)$
Sin2 Ψ	0.046, 0.414, 0.0368, 0.0322, 0.0276, 0.023, 0.0184, 0.0138, 0.0902, 0.0046, 0



Quantification				Refinement Control		
Pattern List		Scan List		Peak List	Anchor Scan Data	
No.	Lin...	Visi...	Name	Start pos...	Omega Position ...	X Positi
1		<input checked="" type="checkbox"/>	SYUFIQA...	55.8231	0.0000	
2		<input checked="" type="checkbox"/>	SYUFIQA...	55.8231	0.0000	
3		<input checked="" type="checkbox"/>	SYUFIQA...	55.8231	0.0000	
4		<input checked="" type="checkbox"/>	SYUFIQA...	55.8231	0.0000	
5		<input checked="" type="checkbox"/>	SYUFIQA...	55.8231	0.0000	
6		<input checked="" type="checkbox"/>	SYUFIQA...	55.8231	0.0000	
7		<input checked="" type="checkbox"/>	SYUFIQA...	55.8231	0.0000	
8		<input checked="" type="checkbox"/>	SYUFIQA...	55.8231	0.0000	
9		<input checked="" type="checkbox"/>	SYUFIQA...	55.8231	0.0000	
10		<input checked="" type="checkbox"/>	SYUFIQA...	55.8231	0.0000	
11		<input checked="" type="checkbox"/>	SYUFIQA...	55.8231	0.0000	
12		<input checked="" type="checkbox"/>	SYUFIQA...	55.8231	0.0000	
13		<input checked="" type="checkbox"/>	SYUFIQA...	55.8231	0.0000	
14		<input checked="" type="checkbox"/>	SYUFIQA...	55.8231	0.0000	
15		<input checked="" type="checkbox"/>	SYUFIQA...	55.8231	0.0000	
16		<input checked="" type="checkbox"/>	SYUFIQA...	55.8231	0.0000	
17		<input checked="" type="checkbox"/>	SYUFIQA...	55.8231	0.0000	
18		<input checked="" type="checkbox"/>	SYUFIQA...	55.8231	0.0000	
19		<input checked="" type="checkbox"/>	SYUFIQA...	55.8231	0.0000	
20		<input checked="" type="checkbox"/>	SYUFIQA...	55.8231	0.0000	
21		<input checked="" type="checkbox"/>	SYUFIQA...	55.8231	0.0000	

(a)



(b)

Figure 3. 9 (a) and (b) The measurement of scan result

The stress determination used is sin² psi method. By placing the sample in the XRD machine and run the stress measurement procedure, the value for d-spacing will be obtained. The theory of linear elasticity will be used to calculate the respective residual stress. The curve of inter-planar spacing will be plotted. Hence, the value residual stress can be measured from the gradient of the graph plotted together with the basic knowledge of the material's elastic properties.

The stress is given by:

$$\sigma_{\phi} = \left(\frac{E}{1+\nu} \right) m \quad (3.1)$$

Where m is the gradient of the graph of d vs. $\sin^2 \psi$, ν is for Poisson Ratio and E is Young Modulus. The positive stress value will represent tensile residual stress and negative value represent compressive residual stress (Fitzpatrick, M. E, 2005)

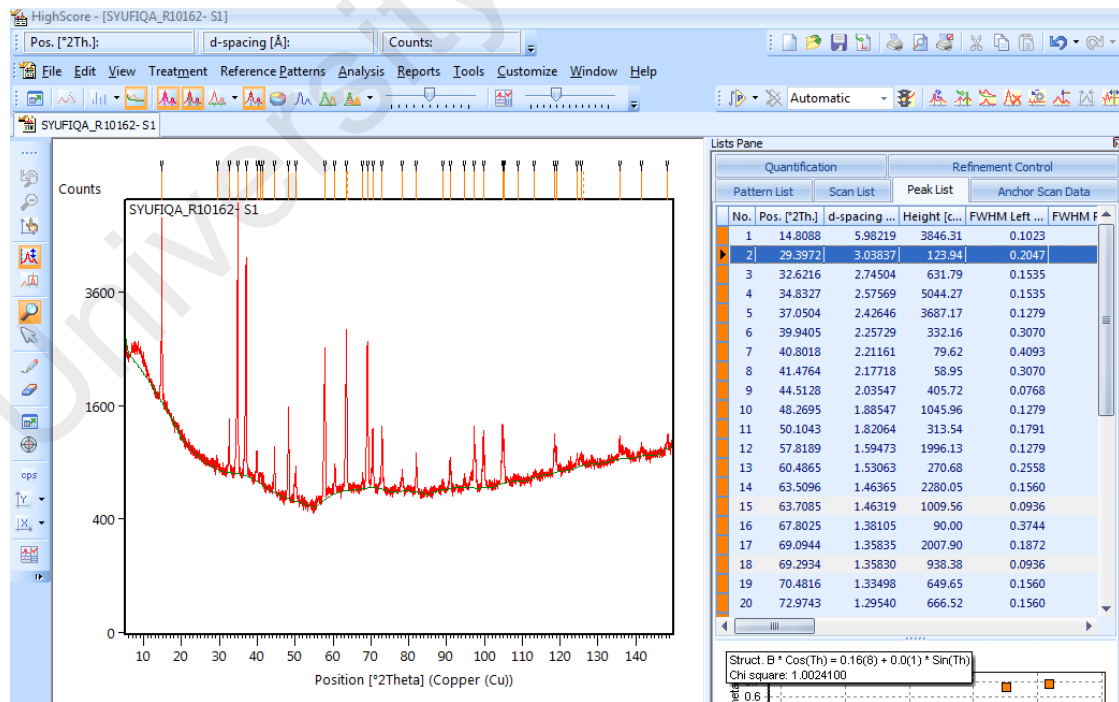
3.4 Grain Measurement

3.4.1 Scherer Equation

For grain size, Scherer Equation method is adopted to calculate the crystallite size for these three samples at chosen peak. The equation is given by:

$$B(2\theta) = \frac{K\lambda}{L \cos \theta} \quad (3.2)$$

Where K is Scherrer Constant, λ is the x-ray wavelength and L is value of Full Width at Half Maximum (FWHM) of XRD peak profile or integral breadth (Mote et.al, 2012). The value of FWHM and integral breadth can be easily obtained from the XRD absolute scan at the chosen peak angle.



(a)

Quantification			Refinement Control		
Pattern List		Scan List	Peak List	Anchor Scan Data	
No.	Pos. [°2Th.]	d-spacing ...	Height [c...	FWHM Left ...	FWHM F
1	14.8088	5.98219	3846.31	0.1023	
2	29.3972	3.03837	123.94	0.2047	
3	32.6216	2.74504	631.79	0.1535	
4	34.8327	2.57569	5044.27	0.1535	
5	37.0504	2.42646	3687.17	0.1279	
6	39.9405	2.25729	332.16	0.3070	
7	40.8018	2.21161	79.62	0.4093	
8	41.4764	2.17718	58.95	0.3070	
9	44.5128	2.03547	405.72	0.0768	
10	48.2695	1.88547	1045.96	0.1279	
11	50.1043	1.82064	313.54	0.1791	
12	57.8189	1.59473	1996.13	0.1279	
13	60.4865	1.53063	270.68	0.2558	
14	63.5096	1.46365	2280.05	0.1560	
15	63.7085	1.46319	1009.56	0.0936	
16	67.8025	1.38105	90.00	0.3744	
17	69.0944	1.35835	2007.90	0.1872	
18	69.2934	1.35830	938.38	0.0936	
19	70.4816	1.33498	649.65	0.1560	
20	72.9743	1.29540	666.52	0.1560	

(b)

Figure 3. 10 (a) and (b) XRD scan and FWHM value for each peak from absolute scan

3.4.2 SEM and EDX

Scanning Electron Microscopy also known as SEM is used in this experiment to observe the grain size. Meanwhile Energy-dispersive x-ray known as EDX is chemical microanalysis technique used in conjunction with SEM. Both of this method use the same machine which is Phenom ProX. Magnification used for SEM is 15000. The SEM will be accomplished by using Element Identification software and EDX by using Phenom ProSuite.

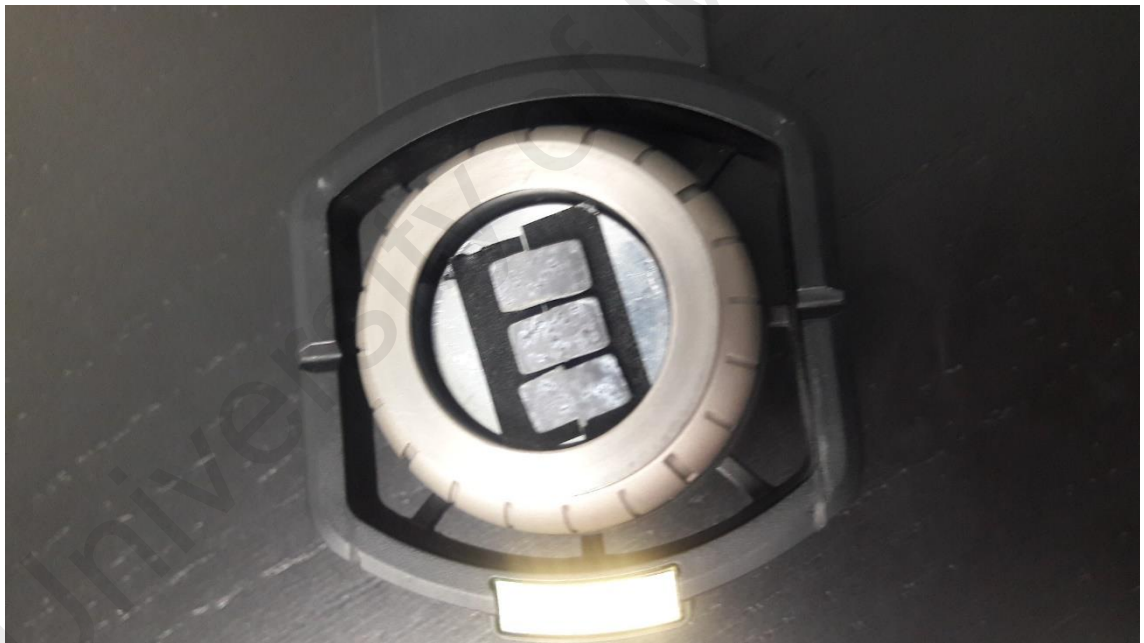


Figure 3. 11 Phenom ProX machine

First, the sample will be stick onto the tool holder and adjusted to suitable height. The blower will blow the sample, so that it will clean up any dust contained inside the sample. Then, the sample will be loaded into the machine.



Figure 3. 12 Tool holder



(a)



(b)

Figure 3. 13 (a) and (b) Samples on the tool holder



Figure 3. 14 Sample loaded into the machine

CHAPTER 4 : RESULTS AND DISSCUSSION

In this chapter, it will be divided into 2 main section which is residual stresses and grain size.

4.1 Residual Stress

4.1.1 Experimental results

After the stress measurement is done by using XRD machine, the d-spacing value is obtained and the graph of d vs. $\sin^2\Psi$ is plotted. Figures below showed the graph plotted for all three samples.

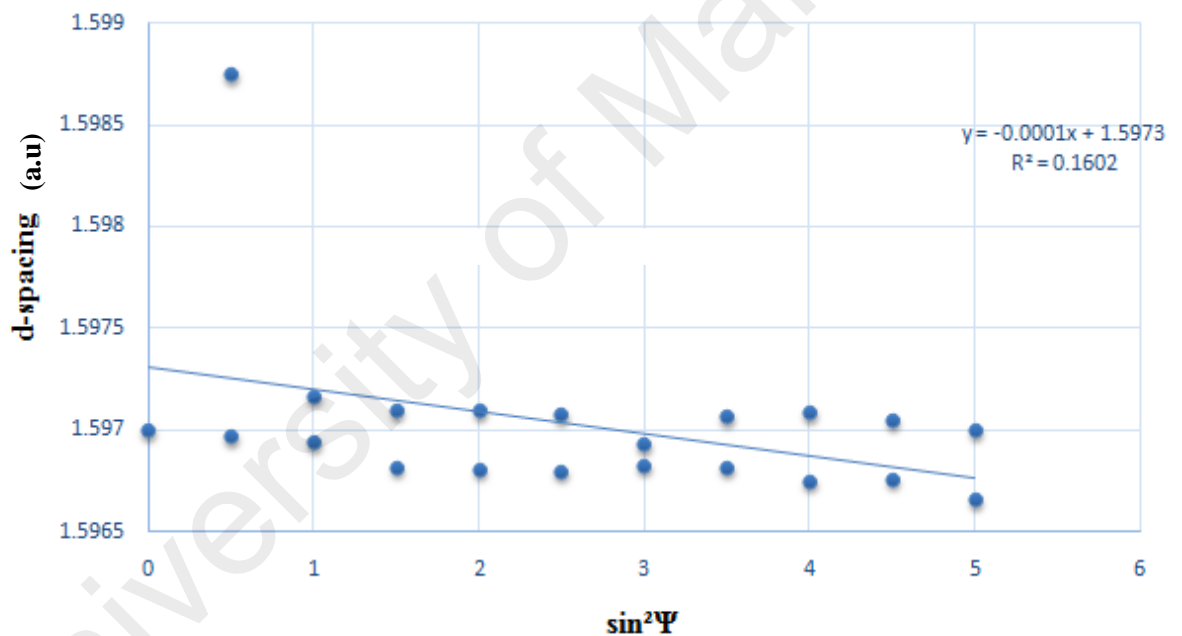


Figure 4. 1Graph d vs. . $\sin^2\Psi$ for sample 1 pass

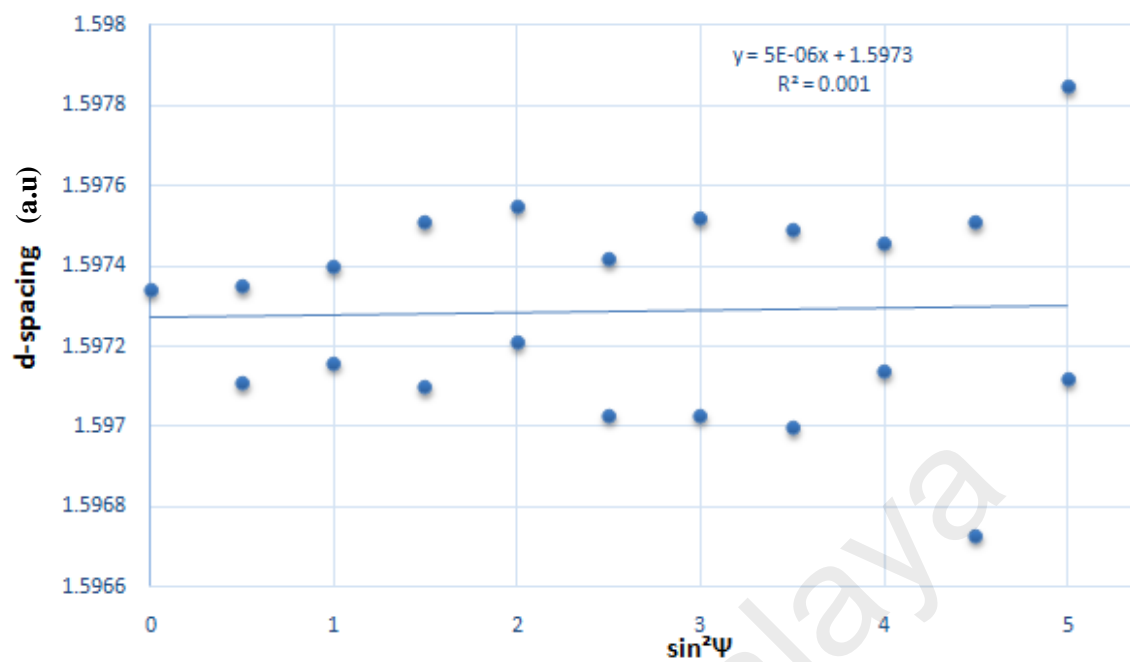


Figure 4. 2Graph d vs. $\sin^2\Psi$ for sample 2 passes

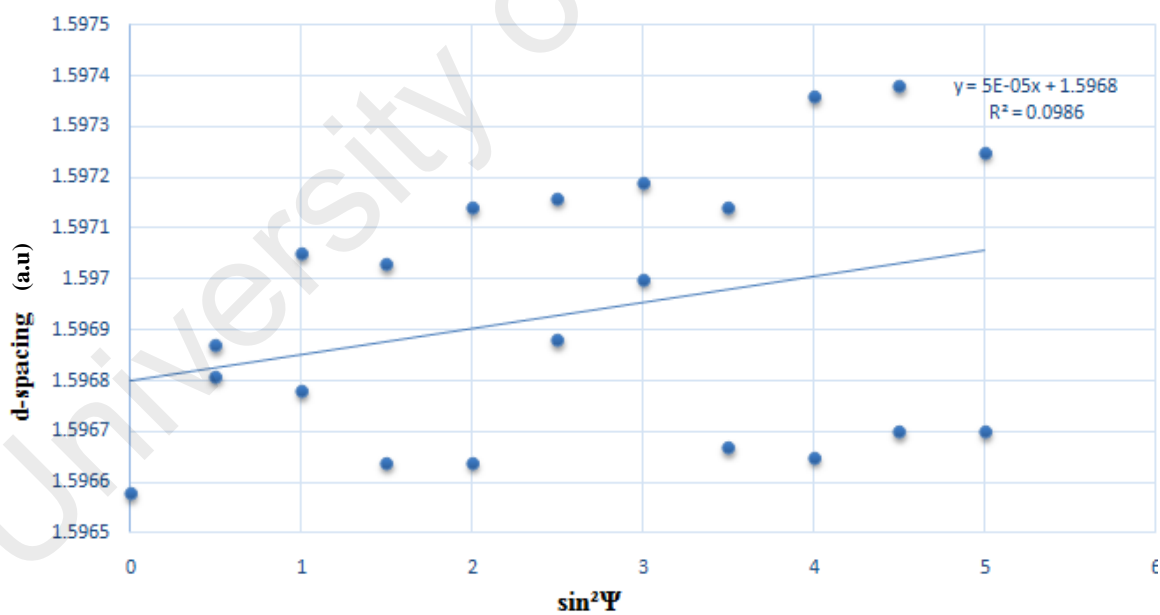


Figure 4. 3Graph d vs. $\sin^2\Psi$ for sample 3 passes

4.1.2 Analysis and discussion

The residual stress can be calculated by using the theory of elasticity. In this theory, the gradient of the graph will be used to calculate the residual stress. All the required value will be substituted into the following equation:

$$\sigma_{\phi} = \left(\frac{E}{1+\nu} \right) m \quad (3.1)$$

Where m is the gradient of the graph of d vs. $\sin^2 \psi$, ν is for Poisson Ratio and E is Young Modulus. The Young Modulus and Poisson's Ratio for Magnesium Alloy ZK60 is 46GPa and 0.35 respectively. The table and the graph below shows the calculated residual stresses for each sample.

Table 4. 1 Residual Stress Measurement Value

Sample (No. of passes)	Residual stresses
1	-33.185KPa
2	+1659.2 KPa
3	+165.92KPa

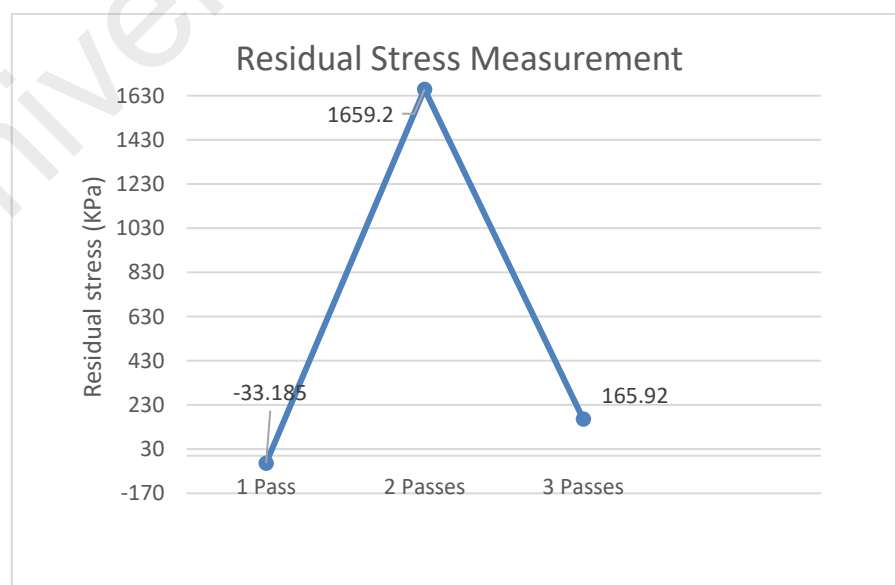


Figure 4. 4 Residual Stress Measurement

From the graph in Figure 4.2, it shows that the residual stress for each sample is significantly different. For sample with 1 pass, the residual stress is negative. Meanwhile the other samples have positive value of residual stresses. This indicates that sample with 1 pass having a compressive residual stress while sample with 2 and 3 passes are having tensile residual stresses. However sample 2 and 3 passes varies differently as sample with 2 passes has much higher positive residual stress compared to sample with 3 passes. In this case, sample with 2 passes has the highest tensile stress which is at 1659.2KPa. The residual stress increase first. However, it decreases at the third pass.

The effect of residual stress may be either detrimental or beneficial. However, it depends upon the sign, magnitude and also distribution of the stress with respect the load that induced stresses (Paawar et.al, 2017). Accessing the quality of the parts by characterizing the residual stress is crucial to ensure the parts performance and lifetime (Zhou et.al, 2014). For sample with 1 pass, it is such an advantage as the compressive residual stress is much more desirable compared to tensile residual stress. It is because the compressive stresses will eventually help the sample to hold together more strongly and not easily breakable. For fatigue crack to initiate, it usually happened on the surface of material due to high and maximum of stresses on the surface. By having a compressive residual stress, the particle are plastically compressed up to certain level. Residual stress is one of the crucial factor that need to be taken into consideration during any components design. It is because it will apply an additional force towards the components and affect the components mechanical behavior. As stated by Tsivoulas et.al (2015), such stresses like negative sign can be an advantage as they apply compressive forces onto the material's surface which helps to inhibits cracking and also prolong the tool life of the part. Hence it will increase the fatigue life and enhance the performance of the material.

For sample with higher amount of tensile residual stress like sample 2 and 3 passes, it is the opposite from the compressive residual stress. It can generate a crack on

the surface of the material much faster and decrease the fatigue life. As stated by Hemmesi et.al (2017), by having large amount of tensile residual stresses, it can be potentially decrease the tolerance of the component against applied external load. The tensile residual stress may also occurred from the multiple deformation on the machined surface (Zhou et.al, 2014). Hence, it will lowered the performance and tool life of the materials. It is normal for this process to have a positive and negative residual stress as this process will lead to additional tensile and compressive strain. It is because the diameter of the tube is changing during this process and it reverts to the initial state at the end of the process (Faraji et.al, 2011).

In year 2014, Sanati et.al investigates the residual stress of Aluminum tube that also been deform by using the same process which is Parallel Tubular Chanel Angular Pressing method. In the experiment, it has been found that most of the residual stresses are negative stress which is compressive stress. They also found that the residual stress value and affected are not changing after the 3rd passes of PTCAP. The gradient of the stress graph also decreasing as the number of passes increase. In contrast, in this experiment the sample with 1 pass of PTCAP is the only one that have the negative value of residual stress. However, the same situation also happened when the gradient of the stress graph also decrease when the number of the passes increase and the residual stress also decrease.

However, all these results of residual stress measurement may also been influence by others external factor and conditions. In this experiment, the sample was cut by using EDM process. Even though EDM cutting only affect the tinniest area of cutting zone, but it still able to alter and distort the initial amount of residual stress on the surface of material. The positioning of the sample inside the XRD machine also may affected the measurement result. As stated earlier, the sample is initially in a hollow tube shape. In order to make it fit the machine, the sample is cut into smaller pieces. But the sample is

still having its curvature shape. It is quite hard to get the x-ray beam to strike the sample accurately on the desired surface as it has some curvature unlike other solid sample like thin film. This may also affect the result for the stress measurement. XRD measurement technique may be one of the most common technique used, however in this case as the sample is not in the flat shape and the geometry is not as simple as thin film. This XRD machine has quite limited area and accessibility for stress measurement. This may lead to error in making measurement.

From the figure 4.1, 4.2 and 4.3, all these graphs showed the distribution of d-spacing for each stress measurement curve. This measurement was made at one particular 2theta angle. In this case, the residual stress measurement was made at peak angle of 58.8199° . For Magnesium Alloy ZK60 which having composition of 94wt% Mg, 4.8-6.2wt% Zn and 0.45wt% Zr, the XRD profile show that the highest peak of intensity is at angle 2Theta between 30° to 40° . However, the highest peak provided two actual peak which make it difficult to perform stress measurement. This particular peak also only provided less number of stress measurement graph, hence provide less number of d-spacing. It is quite challenging to choose the peak for residual stress measurement as all the other peaks are not reliable to do the analysis. The peak chosen must be quite far from another peak and having one particular sharp peak. Many trials have been done on the other peak. However, at 2theta of 58.8199° showing the most consistent result compared to others. In year 2018, Zhang et.al run an experiment of high cycle fatigue behavior of extruded magnesium alloy ZK60. The XRD profile of the magnesium alloy shows that between 2theta 55° to 60° , there is one particular peak that shows the present of magnesium composition at intensity of 5000. Hence, peak can be taken and reliable to do the residual stress measurement even though it is not the highest peak in the XRD profile.

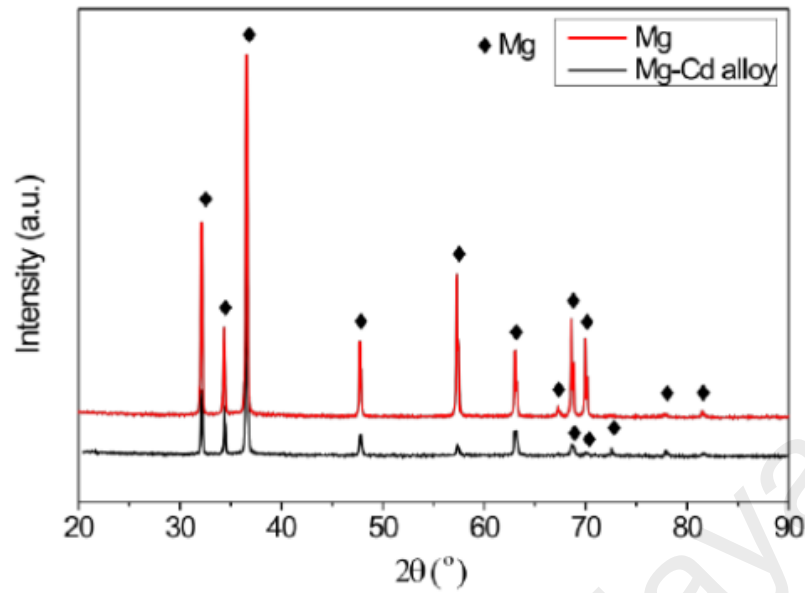


Figure 4. 5 XRD profile of Magnesium Alloy ZK60 (Zhang et.al, 2018)

In the experiment of deformation PTCAP, INSTRON Press Machine with force of 300KN is used. By applying this force onto the sample, the sample was deformed and lead to maximum residual tensile stress at 2 passes which is at 1659.2 KN. It shows that the residual stress remain inside the sample is much higher than the initial applied force.

4.2 Grain Size

4.2.1 Grain size calculated result- Scherrer Method

For the grain size measurement, the Scherrer Equation is adopted as the information in the equation can be directly obtained from the XRD absolute scan for each sample. The Scherrer Equation is given as follow:

$$B(2\theta) = \frac{K\lambda}{\beta \cos\theta} \quad (4.1)$$

All the result for the grain size are tabulated as follow:

Table 4. 2 Grain size measurement

Sample (passes)	$2(\Theta)$	Integral Breadth (β)
1	57.8189	0.1262
2	57.5135	0.1248
3	57.5061	0.1009

Table 4. 3 Grain size calculated value

Sample (passes)	Grain size (nm)
1	75.14
2	75.86
3	93.789

4.2.2 Grain size analysis and discussion

From the tables 4.2 and 4.3 above, the grain size were obtained by applying Scherrer equation and substituting integral breadth value gets from the XRD absolute scan measurement. The integral breadth is used instead of Full Width at Half Maximum (FWHM) because it takes into account the whole shape of the profile. Meanwhile for FWHM, the profile is taken from half of the intensity point by excluding the shoulder and tail area. In this case, the integral breadth decrease as the number of passes increase.

The grain size increases from the first sample with single pass of PTCAP process to the third sample with 3 passes. However, the grain size only increases few numbers from 1 pass to 2 passes. It keeps increasing at the third pass showing that the elongation of the grain is still growing. However, according to G.Faraji et.al (2013) conduct a research using PTCAP method to investigate the dislocation densities and TEM analysis of nanostructured copper tube. From the TEM analysis, it shows that after the first pass the sub grain is elongated together with the interior tangled dislocation were formed.

However, after the second pass the sub grain elongation was decreased. During the third pass, the elongation was almost disappeared. The result also showed that by increasing the number of passes will lead to decrease in dislocation densities. Even though the elongation was almost disappeared, the grain is still increasing to the third pass. Hence, it shows that PTCAP able to increase the size of the grain until its third pass.

4.2.3 Grain size observed result – SEM and EDX

The microstructure analysis is done further by using SEM and EDX on each sample. Pictures below show the result of SEM and EDX on the samples. EDX is measured on one spot for each sample.

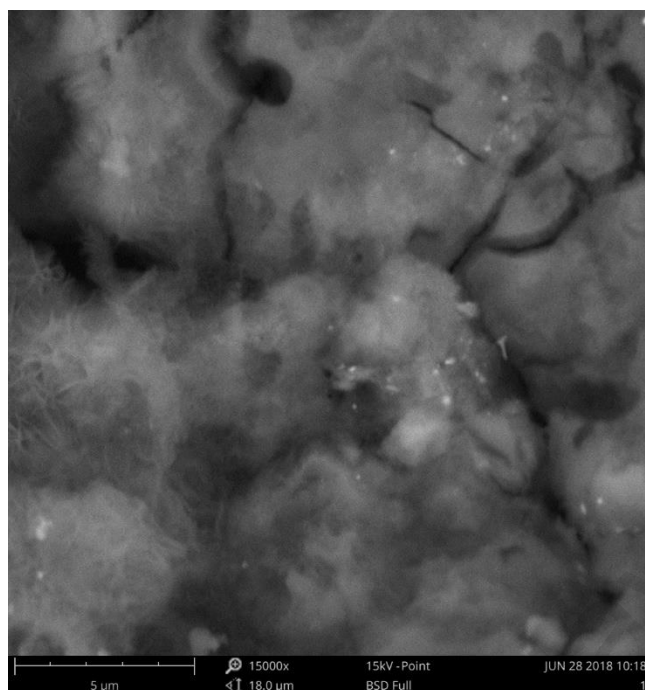


Figure 4. 6 SEM PTCAP 1 pass

Table 4. 4 EDX PTCAP 1 pass

Element Symbol	Atomic Conc.	Weight Conc.	Oxide Symbol	Stoich. wt Conc.
O	71.45	59.55	-	-
Mg	27.69	35.05	Mg	86.66
I	0.57	3.76	I	9.30

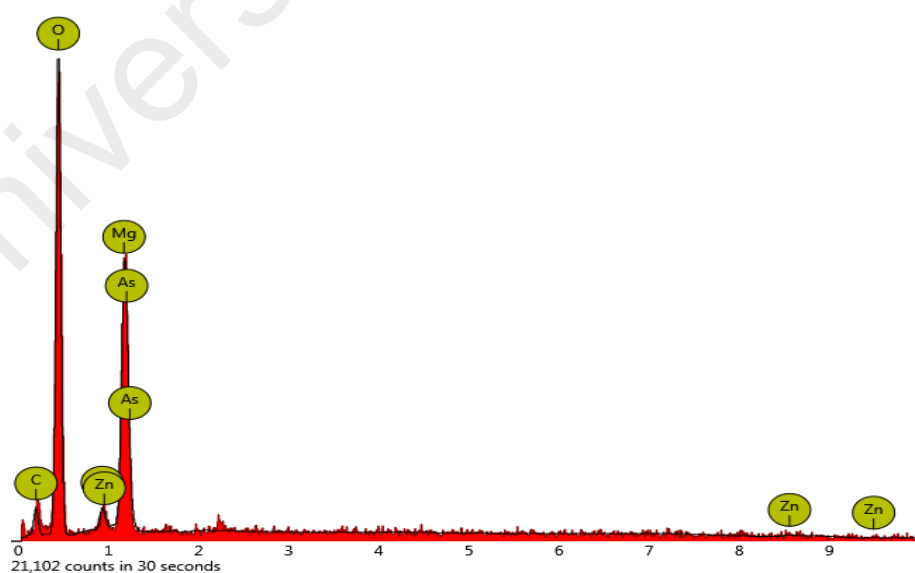


Figure 4. 7 EDX acquisition graph PTCAP 1 pass

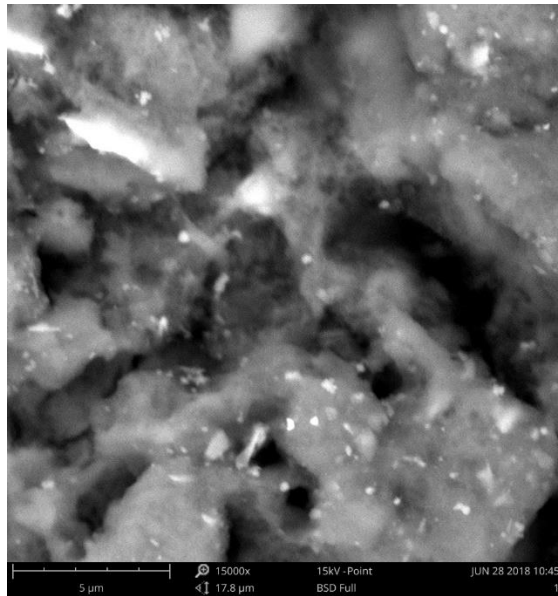


Figure 4. 8 SEM PTCAP 2 passes

Table 4. 5 EDX PTCAP 2 pass

Element Symbol	Atomic Conc.	Weight Conc.	Oxide Symbol	Stoich. wt Conc.
O	55.70	42.70	-	-
C	21.46	12.35	C	21.55
Mg	10.43	12.15	Mg	21.20
Ti	6.38	14.64	Ti	25.55
S	3.98	6.12	S	10.67
La	1.29	8.59	La	14.99
Tc	0.74	3.46	Tc	6.04

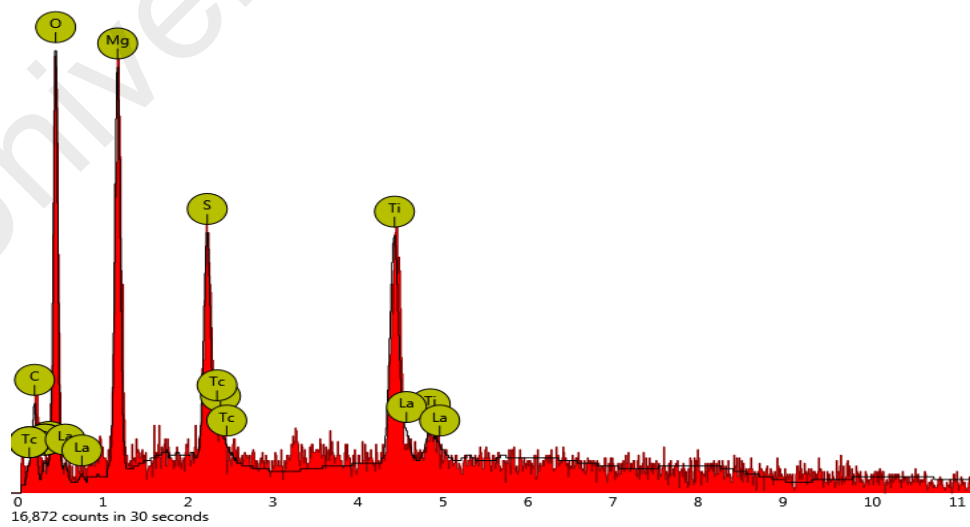


Figure 4. 9 EDX acquisition graph PTCAP 2 pass

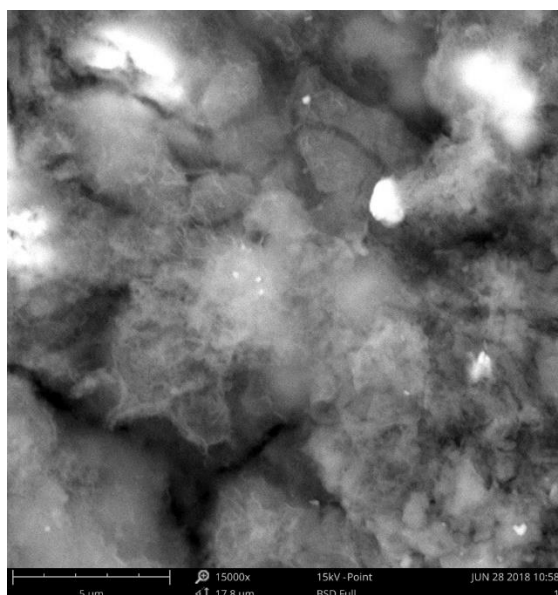


Figure 4. 10 SEM PTCAP 3 passes

Table 4. 6 EDX PTCAP 3 pass

Element Symbol	Atomic Conc.	Weight Conc.	Oxide Symbol	Stoich. wt Conc.
O	67.82	52.02	-	-
Mg	14.21	16.56	Mg	34.51
C	13.50	7.77	C	16.20
S	2.46	3.79	S	7.89
Pb	2.00	19.86	Pb	41.40

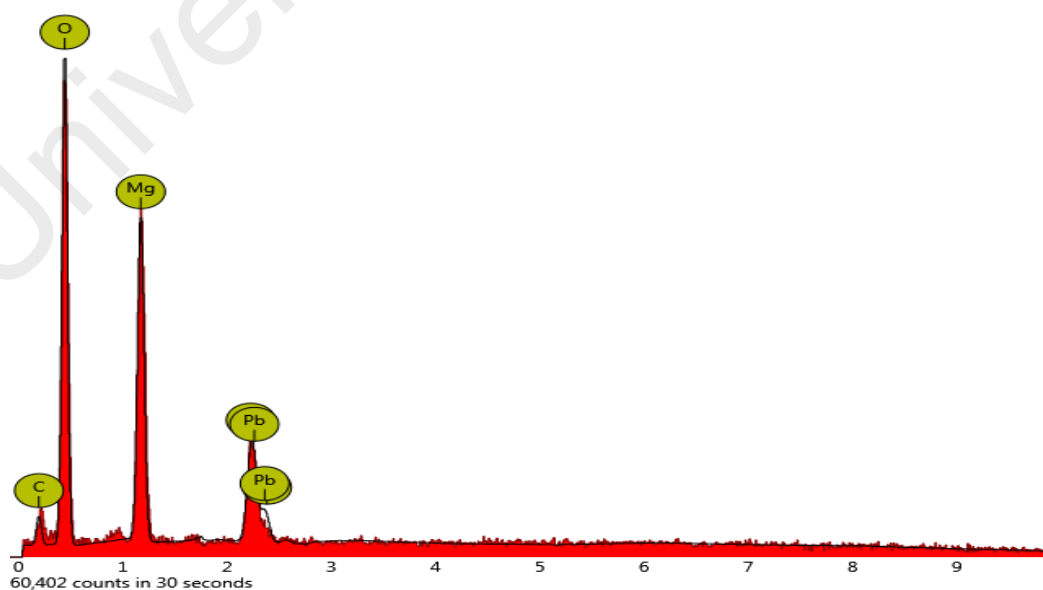


Table 4. 7 EDX acquisition graph PTCAP 3 pass

4.2.4 SEM and EDX result analysis

The SEM image of the samples can be observed from Figure 4.6, 4.8 and 4.10. The image from sample with 1 pass shows that the grain and grain boundary can be easily detected and seen. In fact, the grain is more uniform. Compared to the sample with 2 passes, even though the grain can be seen clearly, however it overlapped with each other and less uniform shape formation of grain. Finally the sample with 3 passes, the image almost the same with the sample with single pass, but the grain boundary is hardly seen and the grain appear much more elongated from the other samples. In year 2014, Stepanov et.al also use SEM analysis to see the microstructure of Equal Channel Angular Pressing (ECAP) process. It said that the grain refinement increase as the number of passes increase. Thus, through SEM, the microstructure of PTCAP can be observed and analyze accordingly. It shows the different between all the grain sizes. However, for the best confirmation, the grain size is calculated by using a tool inside the software where the grain can be directly measured.

Meanwhile, for the EDX analysis, it showed the composition of elements that present on the sample. All three spots taken can be considered as magnesium as can be seen from the acquisition graph. The other elements that exist on that spot can be considered as faults as the percentage is very small. In fact, some of the impurities are already stick onto the sample surface from previous activities. In this experiment, the sample itself is already gone through cutting process and deformation process. So it is possible for other elements to be inside the sample. Thus, it is important to clean and blow the sample first before conduct SEM and EDX.

4.2.5 Grain size observed vs calculated

For a better comparison, the observed and calculated grain size are compared.

The percentage difference is calculated by using formula

$$\Delta D = \frac{|D_{calculated} - D_{observed}|}{D_{observed}} \sim 10\% \quad (4.2)$$

Table 4. 8 Grain size difference

Sample PTCAP	Calculated (nm)	Observe (nm)	% Difference
1 pass	75.14	79.3	5.25
2 pass	75.86	87.8	13.59
3 pass	93.79	104	9.8

From the table above, the percentage difference of the sample of 2 pass is the highest compared to other sample. The observed grain is much bigger than the calculated grain size. Overall, either from calculated or observed result, the grain size is increasing. By increasing the number of passes, it shows a definite grain elongation. The percentage difference may cause from several factors. For instance, the sample itself has some errors during XRD measurement. The machine itself, even though it already been calibrated, there are always errors come from the machine. In fact, the human error also included during installation of the sample.

In this experiment, it has been obvious that by increasing the number of passes, the grain size is also increasing. In this case, most of the material usually will experience grain refinement. However, for magnesium Alloy ZK60, the grain size is getting bigger after few passes. In year 2005, Lapovok et.al has conducted a research to enhance super plasticity of magnesium alloy ZK60 by using one of the SPD method which is Equal Chanel Angular Pressing (ECAP). The finding of the research shows that exceptionally

high tensile ductility is reported when the pressing is done without any extra process. In fact, the grain structure shown is to be bi-modal with many different grain sizes. Meanwhile, in year 2014 Roberto et.al also processed magnesium alloy using SPD method. It is reported that ultrafine-grained structure are obtained in magnesium alloy by multiple pass of ECAP at moderate temperature. Hence, for magnesium alloy, it is important to know the suitable processing temperature in order to get the ultrafine-grained structure. However, in this experiment the sample which in tube shape is annealed at high temperature of 600° for a time period of 1 hour to achieve homogeneous microstructure. This explained the reasons behind the increment in the sample grain size. Recently, Faraji and Amani (2018) also used magnesium alloy but with different grade which is WE43 magnesium alloy that processed via one of the new SPD process which is cyclic expansion extrusion to study the recrystallization and its mechanical properties. The processing temperature and number of passes also investigated. It shown that the bimodal structure with ultrafine-grained structure exist after processing at 400°. The ductility also increases after the second passes. Overall, from the experiment they claimed that by increasing the temperature the elongation of the grain increased even it reduce the strength and microhardness. Even with different grade of magnesium alloy, it shows that the processing temperature gives effect on the elongation of the grain size by increasing the number of passes. Lapovok et.al (2013) also produced another type of magnesium alloy which is Mg-Y-Zn by using ECAP powder compaction method. Microstructure variation and the mechanical properties of the material can be affected by various processing route, especially those involving severe plastic deformation. In the research, the study of microstructure and a billet produced from Mg-Y-Zn alloy powder by ECAP-compaction and annealing was carried out. As a result, a promising thermomechanical processing route leading to high strength and sufficient ductility. As going by definition, ductility is the ability to perform plastic deformation before failure. The main mechanism

in plastic deformation is the slip of dislocation. Anything that can cause the difficulty in it can result in lowering the ductility. Grain boundary is one of the major hurdles to movement of dislocation. In smaller grains, there exists large grain boundary area per unit volume and vice versa. As the number of the dislocation increases, it is hard to make a forward movement hence the fracture become brittle instead of ductile.

The grain size percentage difference may cause from the many different sizes of the grain inside the sample itself while the size of grain keep increasing as the ductility of the sample also increasing by increasing the force which in this case it refers to PTCAP passes.

University of Malaysia

CHAPTER 5 : CONCLUSION AND RECOMMENDATION

From this research project, we can conclude that the residual stress does not depend on the number of passes from PTCAP process. It may vary because of the external factor and conditions. The compressive residual stress is more desirable compared to tensile residual stress as it may shorten and decrease the fatigue life of the components. As the recommendation, the residual stress measurement can be done on several peak 2theta compared to only one peak. However, it takes longer time and cost as the XRD machine need to be conducted by a skillful person. Meanwhile for the grain size, it shows that the size of grain increase by increasing the number of passes. It can be proved by the result of percentage difference from calculated and observed grain size where the percentage of difference is still in the range. The size of the grain keeps increasing by increasing the number of passes because of the result of the ductility of the magnesium alloy itself. Meanwhile, the residual stress and grain size does not show any correlation as the grain size keep increasing even though the value of residual stress change non-uniformly. For further investigation, Electron backscatter diffraction (EBSD) is recommended as it can evaluate and understand the structure, crystal orientation and phase of materials in the Scanning Electron Microscope (SEM). PTCAP for magnesium alloy also can be annealed at few different temperatures to see the effect of annealed temperature to the grain size and its ductility.

REFERENCES

Amani, Soheil & Faraji, Ghader. (2018). Recrystallization and mechanical properties of WE43 magnesium alloy processed via cyclic expansion extrusion. *International Journal of Minerals, Metallurgy, and Materials*. 25. 672-681. 10.1007/s12613-018-1614-7.

B Figueiredo, Roberto & Paulino Aguilar, Maria Teresa & Cetlin, P & G Langdon, Terence. (2014). Processing magnesium alloys by severe plastic deformation. *IOP Conference Series: Materials Science and Engineering*. 63. 012171. 10.1088/1757-899X/63/1/012171.

Chakravarty, S., Sikdar, K., Singh, S. S., Roy, D., & Koch, C. C. (2017). Grain size stabilization and strengthening of cryomilled nanostructured Cu 12 at% Al alloy. *Journal of Alloys and Compounds*, 716, 197-203.

Chen, H., Yao, Y. L., Kysar, J. W., Noyan, I. C., & Wang, Y. (2005). Fourier analysis of X-ray micro-diffraction profiles to characterize laser shock peened metals. *International Journal of Solids and Structures*, 42(11-12), 3471-3485.

Tsivoulas, D., Fonseca, J. Q., Tuffs, M., & Preuss, M. (2015). Effects of flow forming parameters on the development of residual stresses in Cr–Mo–V steel tubes. *Materials Science and Engineering: A*, 624, 193-202.

Darling, K., Roberts, A., Mishin, Y., Mathaudhu, S., & Kecskes, L. (2013). Grain size stabilization of nanocrystalline copper at high temperatures by alloying with tantalum. *Journal of Alloys and Compounds*, 573, 142-150.

Faraji, G., Mashhadi, M., Bushroa, A., & Babaei, A. (2013). TEM analysis and determination of dislocation densities in nanostructured copper tube produced via parallel tubular channel angular pressing process. *Materials Science and Engineering: A*, 563, 193-198.

Faraji, G., Babaei, A., Mashhadi, M. M., & Abrinia, K. (2012). Parallel tubular channel angular pressing (PTCAP) as a new severe plastic deformation method for cylindrical tubes. *Materials Letters*, 77, 82-85.

Fitzpatrick, M. E. (2005). *Determination of residual stresses by X-ray diffraction: Issue 2*. Teddington: National Physical Laboratory.

Foadian, F., Carradó, A., & Palkowski, H. (2015). Precision tube production: Influencing the eccentricity and residual stresses by tilting and shifting. *Journal of Materials Processing Technology*, 222, 155-162.

Hajyakbary, F., Sietsma, J., Böttger, A. J., & Santofimia, M. J. (2015). An improved X-ray diffraction analysis method to characterize dislocation density in lath martensitic structures. *Materials Science and Engineering: A*, 639, 208-218.

Hemmesi, K., Farajian, M., & Boin, M. (2017). Numerical studies of welding residual stresses in tubular joints and experimental validations by means of x-ray and neutron diffraction analysis. *Materials & Design*, 126, 339-350.

Lapovok, Rimma & Ng, Hoi & Nie, J.F. & Estrin, Yuri & Mathaudhu, Suveen. (2013). Study of Mg-Y-Zn rod produced by ECAP powder compaction. Materials Science and Technology Conference and Exhibition 2013, MS and T 2013. 2. 1414-1422

Lapovok, R., Cottam, R., Thomson, P., & Estrin, Y. (2005). Extraordinary Superplastic Ductility of Magnesium Alloy ZK60. *Journal of Materials Research*, 20(6), 1375-1378

Longhui, M., Ning, H., Yinfei, Y., & Wei, Z. (2015). Measurement of Surface Residual Stresses Generated by Turning Thin-Wall Ti6Al4V Tubes Using Different Cutting Parameters. *Rare Metal Materials and Engineering*, 44(10), 2381-2386.

Mahur, B. P., Bhardwaj, Y., & Bansal, V. (2017). Review on finite element analysis for estimation of residual stresses in welded structures. *Materials Today: Proceedings*, 4(9), 10230-10234.

Marinkovic, B., Avillez, R. R., Saavedra, A., & Assunção, F. C. (2001). A comparison between the Warren-Averbach method and alternate methods for X-ray diffraction microstructure analysis of polycrystalline specimens. *Materials Research*, 4(2), 71-76.

Mesbah, M., Fadaeifard, F., Karimzadeh, A., Nasiri-Tabrizi, B., Rafieerad, A., Faraji, G., & Bushroa, A. R. (2016). Nano-mechanical properties and microstructure of UFG brass tubes processed by parallel tubular channel angular pressing. *Metals and Materials International*, 22(6), 1098-1107.

Mohd, M. H., Lee, B. J., Cui, Y., & Paik, J. K. (2015). Residual strength of corroded subsea pipelines subject to combined internal pressure and bending moment. *Ships and Offshore Structures*, 1-11.

Mote, V., Purushotham, Y., & Dole, B. (2012). Williamson-Hall analysis in estimation of lattice strain in nanometer-sized ZnO particles. *Journal of Theoretical and Applied Physics*, 6(1), 6

Practical Residual Stress Measurement Methods. (2013).

Rao, P. S., Ramji, K., & Satyanarayana, B. (2016). Effect of wire EDM conditions on generation of residual stresses in machining of aluminum 2014 T6 alloy. *Alexandria Engineering Journal*, 55(2), 1077-1084.

Rao, P. S., Ramji, K., & Satyanarayana, B. (2016). Effect of wire EDM conditions on generation of residual stresses in machining of aluminum 2014 T6 alloy. *Alexandria Engineering Journal*, 55(2), 1077-1084.

Reyes-Ruiz, C., Figueroa, I., Braham, C., Cabrera, J., Zanellato, O., Baiz, S., & Gonzalez, G. (2016). Residual stress distribution of a 6061-T6 aluminum alloy under shear deformation. *Materials Science and Engineering: A*, 670, 227-232.

Silverstein, R., & Eliezer, D. (2017). Effects of residual stresses on hydrogen trapping in duplex stainless steels. *Materials Science and Engineering: A*, 684, 64-70.

Simm, T., Withers, P., & Fonseca, J. Q. (2016). An evaluation of diffraction peak profile analysis (DPPA) methods to study plastically deformed metals. *Materials & Design*, 111, 331-343. doi:10.1016/j.matdes.2016.08.091

Simm, T., Withers, P., & Fonseca, J. Q. (2016). An evaluation of diffraction peak profile analysis (DPPA) methods to study plastically deformed metals. *Materials & Design*, 111, 331-343.

Stepanov, N. D., Kozin, A. N., Salishchev, G. A., Khlebova, N. E., & Pantsyrny, V. I. (2014). Effect of ECAP on microstructure and mechanical properties of Cu-14Fe

microcomposite alloy. IOP Conference Series: Materials Science and Engineering, 63, 012098.

Pawar, S., Salve, A., Chinchani, S., Kulkarni, A., & Lamdhade, G. (2017). Residual Stresses during Hard Turning of AISI 52100 Steel: Numerical Modelling with Experimental Validation. *Materials Today: Proceedings*, 4(2), 2350-2359.

Tavakkoli, V., Afrasiab, M., Faraji, G., & Mashhadi, M. (2015). Severe mechanical anisotropy of high-strength ultrafine grained Cu–Zn tubes processed by parallel tubular channel angular pressing (PTCAP). *Materials Science and Engineering: A*, 625, 50-55. doi:10.1016/j.msea.2014.11.085

Tsivoulas, D., Fonseca, J. Q., Tuffs, M., & Preuss, M. (2015). Effects of flow forming parameters on the development of residual stresses in Cr–Mo–V steel tubes. *Materials Science and Engineering: A*, 624, 193-202

Ungár, T., Révész, Á., & Borbély, A. (1998). Dislocations and Grain Size in Electrodeposited Nanocrystalline Ni Determined by the Modified Williamson–Hall and Warren–Averbach Procedures. *Journal of Applied Crystallography*, 31(4), 554-558.

Wang, C., Jiang, C., Zhao, Y., Chen, M., & Ji, V. (2017). Surface mechanical property and residual stress of peened nickel-aluminum bronze determined by in-situ X-ray diffraction. *Applied Surface Science*, 420, 28-33

Withers, P. J. (2007). Residual stress and its role in failure. *Reports on Progress in Physics*, 70(12), 2211-2264

Yi, J., Li, X., Ding, J., & Seet, H. (2007). Study of the grain size, particle size and roughness of substrate in relation to the magnetic properties of electroplated permalloy. *Journal of Alloys and Compounds*, 428(1-2), 230-236.

Zhang, Z., Zhou, F., & Lavernia, E. J. (2003). On the analysis of grain size in bulk nanocrystalline materials via x-ray diffraction. *Metallurgical and Materials Transactions A*, 34(6), 1349-1355.

Zhou, J., Bushlya, V., Peng, R. L., Chen, Z., Johansson, S., & Stahl, J. E. (2014). Analysis of Subsurface Microstructure and Residual Stresses in Machined Inconel 718 with PCBN and Al₂O₃-SiCw Tools. *Procedia CIRP*, 13, 150-155.

Zhang, L., Zhang, W., Chen, W., & Wang, W. (2018). Cyclic hardening behavior of extruded ZK60 magnesium alloy with different grain sizes.

University of Malaya